Utah Vehicle Electrification Air Quality and Health Impacts

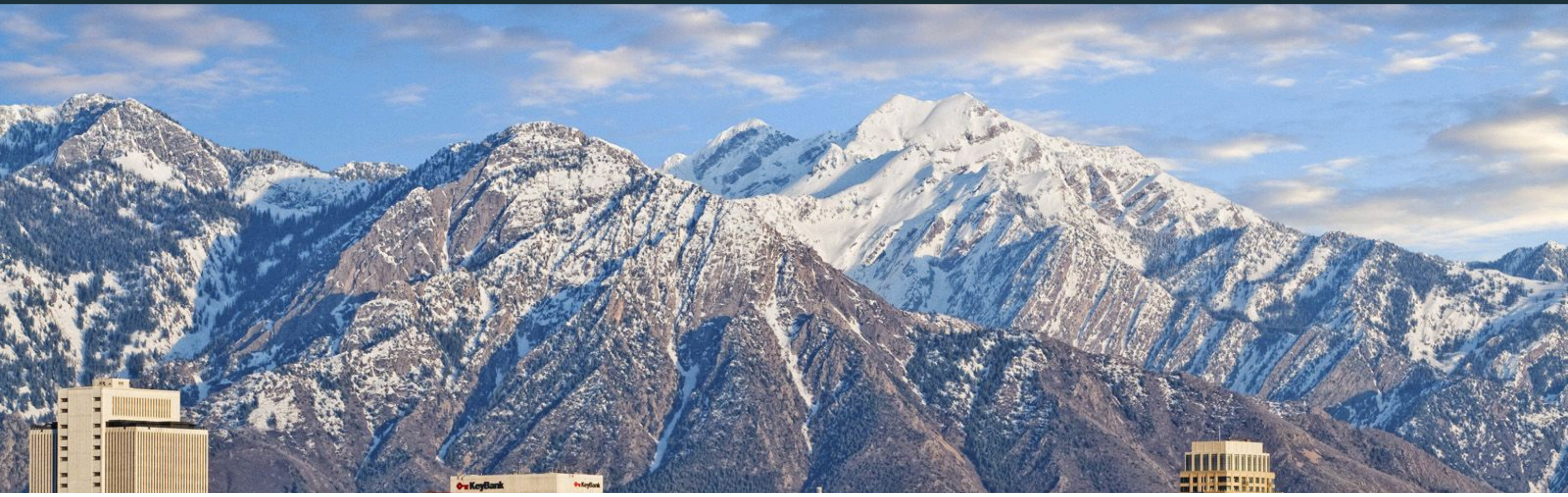

Executive Summary

This project considered the air pollution impact of 18 emissions scenarios—0%, 60%, and 100% vehicle electrification (EV) with added load powered by 0%, 40% and 80% renewable energy (RE) for 2025, 2035, and 2045—run through InMAP, a reduced-complexity air quality model, to estimate the changes in PM2.5 and NO2 concentrations compared to a baseline scenario. All scenarios resulted in net improvements in PM2.5 and NO2 concentrations. The 60% EV adoption scenarios delivered lower reductions in air pollution concentrations compared to the 100% vehicle electrification scenarios. Reductions in PM2.5 and NO2 concentrations increased in future decades due to projected increases in population and onroad emissions in the state. Different assumptions about the power sector—for example, whether added load due to EVs was powered by 0% or 80% renewable energy—had a negligible impact on air pollution concentrations for either PM2.5 or NO2, although it is worth noting that the scenarios with the highest potential to negatively impact air pollution concentrations—100% vehicle electrification with added load met by 0% renewable energy—assume that a substantial portion of added load associated with vehicle electrification is met by power plants in Wyoming, from 31% (2045) to 41% (2025), and that a majority of the added load met within the state of Utah is met by natural gas plants, from 54% (2025) to 70% (2045), instead of coal-fired power plants. These results are *not* universal and are sensitive to the underlying assumptions about the power generation mix—which impacts the quantity and type of pollutants release—and *where* power generation sites are located. Increased reliance on coal fired power generation or construction of new natural gas plants could decrease the positive air pollution impacts observed here, and potentially even lead to adverse health impacts in some locations.

We conducted a health impact analysis (HIA) to explore how these projected changes in air pollution concentrations might translate into changes in deaths and disease onset for all-cause mortality and 11 health endpoints: asthma,

chronic obstructive pulmonary disorder, ischemic heart disease events, stroke, type 2 diabetes, dementia, autism, lung cancer, asthma, acute lower respiratory infection. Each vehicle electrification scenario resulted in hundreds of avoided deaths and disease onset for respiratory diseases (e.g., COPD, asthma), dementia, autism, and diabetes. By 2045, this could equate to 311 cases of avoided COPD, 143 avoided cases of dementia, and 118 cases of avoided childhood asthma onset. Over a decade, vehicle electrification could lead to over 700 and 1,000 avoided deaths from reduced NO2 and PM2.5 exposure, respectively, based on 2025 emissions, or over 1,100 and 1,700 deaths from reduced NO2 and PM2.5 exposure, respectively, based on 2045 emissions. Avoided deaths associated with reductions in NO2 and PM2.5 cannot be added together because the functions we apply to estimate projected health outcomes were derived for each pollutant separately and summing avoided deaths would result in double counting. We did not observe any differences in the modeled health impacts associated with vehicle electrification scenarios based on differences in the amount of renewable energy in the power sector (0% RE, 40% RE, 80% RE), although this could have been influenced in part by assumptions in the power sector modeling (described above). Even when the power sector did produce increases in PM2.5 and NO2 concentrations, these were mitigated by parallel decreases in PM2.5 and NO2 concentrations, even in areas near power plants. As a result, we did not observe any adverse health impacts associated with any vehicle electrification scenario. As with air pollution, the magnitude of modeled health impacts was greater for 100% compared to 60% EV scenarios and increased in scenarios for future decades. This indicates that vehicle electrification might lead to avoided deaths and disease onset in Utah provided that vehicle adoption and electricity generation looks very similar to the scenarios explored here.

1 Methodology

1.1 Transportation Emissions Modeling

1.1.1 Background and Purpose

A key motivation for transportation electrification in Utah is reducing emissions to support improved air quality and health outcomes. The primary emissions-system effects of electrification are twofold: reduced tailpipe emissions and increased grid-related emissions from additional electricity demand.

Because air-quality response is local, the emissions inputs must be spatially disaggregated. This section documents the transportation emissions and transport-electricity-demand modeling used for the annual report. Companion sections document downstream modeling of grid emissions, air quality, and health outcomes.

1.1.2 Modeling Approach

The modeling approach combines:

- vehicle movement and truck-share information by roadway segment,
- pollutant emission factors for passenger and commercial vehicles,
- county-level emissions inventory totals for calibration,
- EV energy-intensity assumptions (kWh/mile), and
- population projections as a proxy for long-run travel-demand growth.

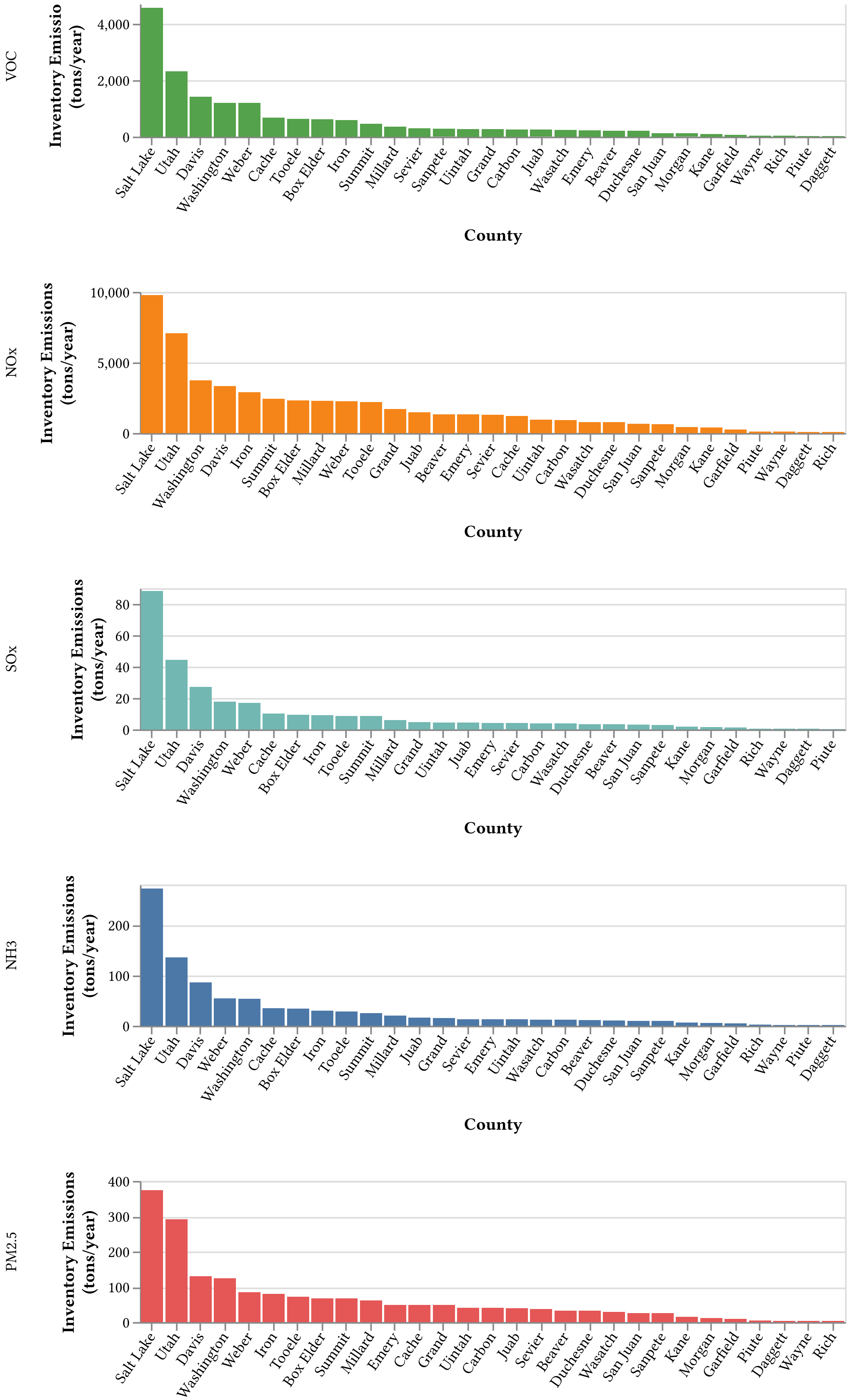

Figure 1: County-level emissions inventory totals by pollutant from the 2019 UDAQ calibration reference.

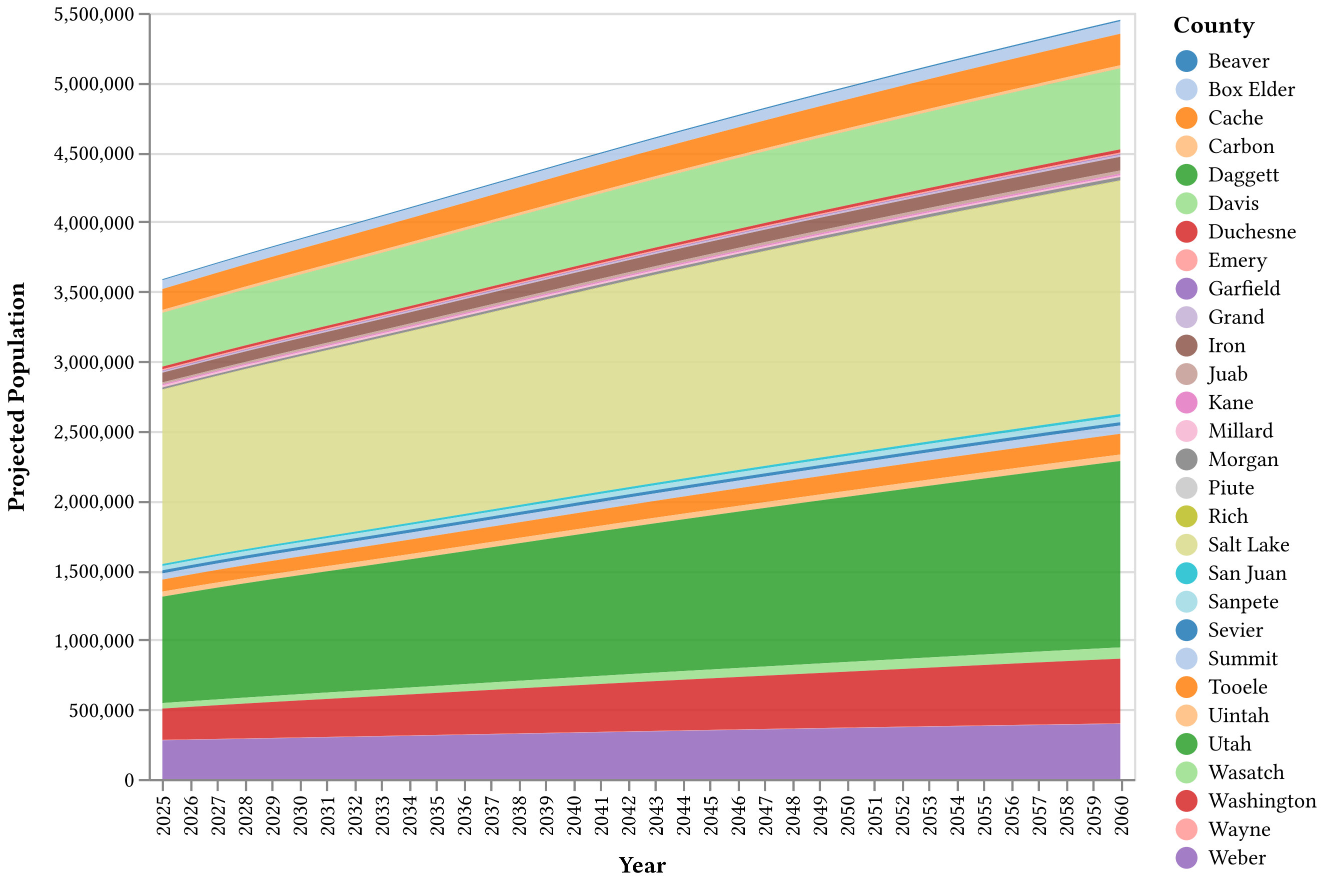

Figure 2: County-level population projections used for demand-growth scaling (Gardner projections).

Together, these inputs produce scenario-based estimates of transportation emissions and electricity demand by year and electrification level.

1.1.3 Data Sources

Key data sources include:

- UDOT roadway movement and truck-share information (through 2025) for road-segment-level activity,
- emissions factor sources used in the transportation model stack (including MOVES-/EMFAC-/GREET-derived inputs embedded in the project pipeline),
- 2019 UDAQ county-level emissions inventory totals for calibration reference (Figure 1),
- EV energy-intensity assumptions for light-duty and heavy-duty fleets, and
- Gardner Policy Institute population projections used as demand-growth multipliers (Figure 2).

1.1.4 Scenario Set

A full-factorial experiment is conducted: 5 modeled years and 6 electrification levels result in 30 total scenarios. Although 100 percent electrification is not a plausible near-term outcome for most modeled years, it is intentionally included to isolate electrification-penetration effects from demand-growth effects along a consistent scenario axis.

Dimension	Values used
Modeled years	2019, 2022, 2025, 2035, 2045
Electrification levels	0, 20, 40, 60, 80, 100 percent
Electrification structure	Equal light-duty and heavy-duty adoption within each scenario

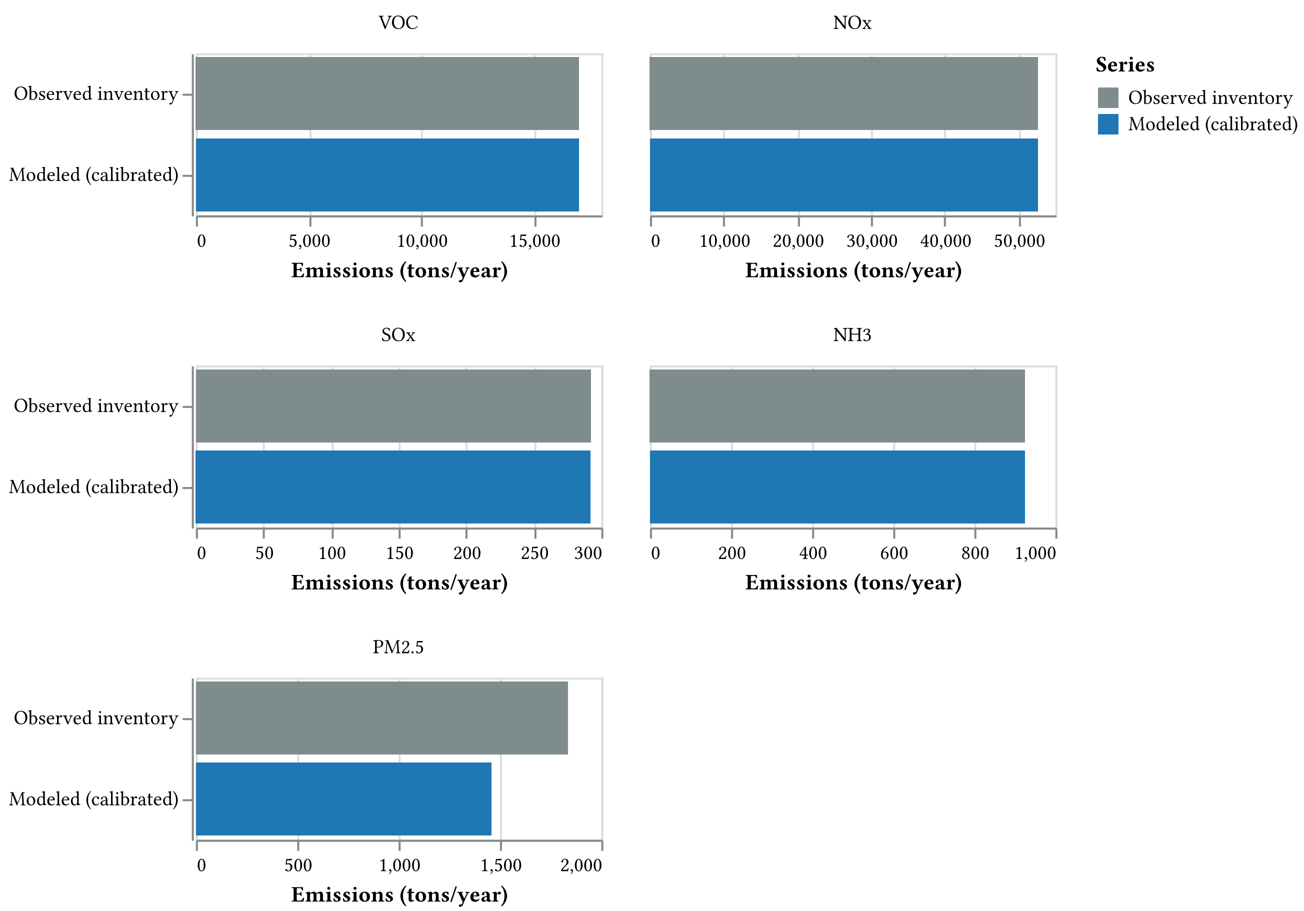

Figure 3: Statewide calibration check in 2019: modeled (calibrated) versus observed inventory totals, shown by pollutant with independent x-axis scales.

Dimension	Values used
Pollutants	VOC, NOx, SOx, NH3, PM2.5
Spatial output	Gridded emissions fields for downstream air-quality modeling
Energy output	Statewide transport electricity demand (TWh/year)

1.1.5 Validation and Verification

Model emission factors (used to estimate emissions from vehicle miles traveled) are calibrated using the 2019 UDAQ inventory and 2019 movement inputs. The modeled-versus-observed calibration comparison is shown in Figure 3.

1.2 Power Systems Emissions Modeling

This section describes the power-systems methods used to translate projected electric-vehicle charging electricity demand into changes in emissions at existing power plants. The method is intentionally simple and transparent: plant data comes from the U.S. Energy Information Administration (EIA), emissions data comes from the U.S. Environmental Protection Agency (EPA), added emitting generation is assigned to existing matched power plants, and each plant's EPA emissions records are scaled in proportion to the new assigned generation.

The outcome of the analysis is a set of scenario-specific emissions inventories. Each inventory reflects the projected charging load for a given year, electrification scenario, and grid scenario, with

Table 1: Matched PACE-region plants used in the emissions scaling analysis. Code is the EIA plant code; baseline, limit, and headroom are annual values. Baseline generation is from the 2017 EIA annual generation data, and the annual limit is estimated from EIA summer and winter net capacity.

Code	Plant	State	Baseline [GWh]	Limit [GWh]	Headroom [GWh]
7790	Bonanza	UT	3,401	3,908	508
56102	Currant Creek	UT	1,193	4,511	3,318
4158	Dave Johnston	WY	4,520	6,248	1,728
3648	Gadsby	UT	93	2,972	2,879
6165	Hunter	UT	8,582	11,343	2,761
8069	Huntington	UT	5,400	7,565	2,165
8066	Jim Bridger	WY	11,643	17,634	5,992
56237	Lake Side Power Plant	UT	3,341	9,954	6,613
4162	Naughton	WY	4,741	5,026	286
50951	Sunnyside Cogen Associates	UT	414	424	10
55622	West Valley Generation Project	UT	122	1,637	1,515
6101	Wyodak	WY	2,565	2,777	212

emissions increased at the existing plants that are assigned the additional emitting generation.

1.2.1 Source Data

The power plant inventory is built from EIA electricity datasets. The analysis uses EIA operating generator capacity data to identify generators in the PACE balancing authority region and retain generators with operating status in 2026 or later. These records provide plant identifiers, plant names, state, balancing authority, and summer and winter net capacity. The analysis also uses EIA annual facility-fuel generation data for 2017 to estimate baseline annual generation at the plant level.

The EPA emissions input is the 2017 National Emissions Inventory point-source electric generating unit dataset, including both continuously monitored and non-continuously monitored electric generating units.

These EPA records contain plant, unit, pollutant, annual emissions, and monthly emissions fields. The analysis joins the EIA and EPA records using the EIA plant code and EPA ORIS facility code. Plants without a corresponding EPA EGU record are not included in the scaled scenario emissions outputs used for this analysis.

The direct EIA-to-EPA match identified 12 emitting plants in the PACE region. Together, those matched plants represented about 46 TWh of baseline annual generation and an estimated 74 TWh annual generation limit, leaving about 28 TWh of available annual headroom under the capacity-limit approximation used in the allocation step. The matched plants are shown in Table 1.

1.2.2 Scenario Load

The scenario electricity demand comes from the statewide grid-energy scenario dataset for the combined light-duty and heavy-duty vehicle case. Each scenario provides an annual statewide charging electricity demand in kWh. The grid scenario is represented as the share of that load supplied by non-emitting generation. Therefore, the additional emitting generation assigned to power plants is

$$E_{\mathrm{emit},s} = \frac{E_{\mathrm{load},s}}{1000}\left(1 - \frac{g_s}{100}\right), \tag{1}$$

where $E_{\text{emit},s}$ is the added emitting generation for scenario s in MWh, $E_{\text{load},s}$ is the annual charging electricity demand in kWh, and g_s is the grid scenario value in percent. A grid scenario of 100 therefore assigns no additional load to emitting plants, while a grid scenario of 0 assigns the full scenario load to emitting plants.

1.2.3 Plant Allocation

For each matched plant, the analysis starts with its EIA baseline annual generation. It also estimates an annual maximum generation level from EIA summer and winter net capacity. The annual limit is calculated from a capacity-weighted year with five summer months and seven winter months, multiplied by a 95% availability factor:

$$G_i^{\max} = 0.95\left(\frac{5P_i^{\text{summer}} + 7P_i^{\text{winter}}}{12}\right)8760, \tag{2}$$

where $G_i^{\max}$ is the estimated maximum annual generation for plant i, P_i^{summer} is the plant's net summer capacity, and P_i^{winter} is the plant's net winter capacity.

The allocation model then solves for a generation scale factor for each plant. The scale factor is constrained to be at least 1, so no emitting plant is assigned less generation than its baseline value. Each plant's scaled generation is also constrained to remain below its estimated annual generation limit. Across all plants, the scaled generation must be at least the baseline generation plus the scenario's added emitting generation.

In simplified form, the model chooses scale factors x_i by solving

$$\min_x \max_i x_i \tag{3}$$

subject to

$$x_i \geq 1, \tag{4}$$

$$x_i G_i \leq G_i^{\max}, \tag{5}$$

and

$$\sum_i x_i G_i \geq \sum_i G_i + E_{\text{emit},s}, \tag{6}$$

where G_i is baseline annual generation for plant i. This formulation spreads the additional emitting generation across the existing emitting fleet as evenly as possible in relative terms. If all plants have enough headroom, they receive a similar proportional increase. If some plants reach their annual generation limits, the remaining added generation is assigned to plants with additional available headroom.

1.2.4 Emissions Scaling

The result of the allocation step is a plant-specific scale factor. That scale factor is applied to the EPA NEI emissions rows for the same facility. The annual emissions value and all monthly emissions values are multiplied by the plant's scale factor:

$$M'_{i,p,m} = x_i M_{i,p,m}, \tag{7}$$

where $M_{i,p,m}$ is the original emissions value for plant i, pollutant p, and month m, and $M'_{i,p,m}$ is the scenario-scaled value. This same proportional scaling is applied to each pollutant and to both annual and monthly emissions columns.

For each year, electrification scenario, and grid scenario, the method produces a scenario-specific emissions inventory. The inventory retains the EPA plant, unit, location, pollutant, and temporal emissions structure, but replaces the baseline emissions values for matched plants with the scenario-scaled values. These scenario inventories are then used as the emissions inputs for the downstream air quality analysis.

1.2.5 Limitations

The primary limitation is that the emitting generation fleet is held fixed. The analysis assumes no new emitting plants are built and no currently emitting plants retire between the baseline data year and the projected load year. If a new emitting plant is built before the projected load occurs, it could take some of the added generation that this analysis assigns to existing plants. Similarly, if an existing emitting plant retires, the added generation would have to be reallocated to the remaining fleet. Either change could alter both the quantity and location of emissions, and therefore the air quality impacts.

The method also uses annual generation and annual plant capacity rather than a chronological dispatch model. It does not simulate hourly power-system operations, transmission constraints, unit commitment, fuel prices, generator ramping, or seasonal outage schedules. As a result, the allocation should be interpreted as a scenario-level emissions scaling method, not as a detailed production-cost simulation.

Emissions are assumed to scale linearly with assigned generation. This means the method does not represent changes in heat rate, pollution-control performance, startup and shutdown behavior, or operating regime as plants move to higher utilization. For annual scenario screening this is transparent and reproducible, but it may understate or overstate emissions changes for individual units if their marginal emissions rates differ from their average baseline emissions rates.

The plant-level scaling approach can also overstate emissions for mixed-fuel plants. Some plants contain multiple generators or units that use different fuels, including secondary units that operate infrequently or only under specific conditions. Because the generation assignment is made at the plant level, the emissions records for all matched units and fuel sources at a plant are scaled uniformly. If the actual increase in generation would come from only a subset of the units at a mixed-fuel plant, this method may incorrectly increase emissions from units or fuels that would not actually serve the added load.

Finally, the method only scales EPA EGU records that can be matched to the EIA plant allocation table. Any missing, mismatched, or incorrectly coded plant identifiers in the source data can affect which plants appear in the scenario inventory and how added generation is distributed.

1.3 Air Quality Modeling

1.3.1 A Primer on Air Pollution Modeling and the Intervention Model for Air Pollution (InMAP)

Changes in emissions do not map neatly onto changes in air pollution concentrations. This transformation is governed by myriad physical forces and chemical reactions occurring in the atmosphere. Air pollution models help bridge this gap, translating changes in emissions inventories into estimated changes in pollution concentrations.

Chemical transport models (CTMs) are air pollution models that simulate three-dimensional chemical reactions and physical transport of pollutants through the atmosphere using meteorology data, emissions inventories, and mathematical equations (Anenberg et al., 2016). They represent the “gold standard” of air quality modeling in terms of their ability to accurately reproduce these complex processes for both gas-phase pollutants (VOCs, NH_3, SO_x, NO_x) and particles, including particulate matter ($PM_{2.5}$). Reduced complexity models (RCMs) use mathematical abstractions derived from CTMs to simulate the relationship between air pollution sources and receptor locations (Anenberg et al., 2016). RCMs are less accurate than CTMs, but they are much less computationally intensive (Anenberg et al., 2016; Baker et al., 2020). Goodkind et al. (2019) found that their RCM modeling required approximately 15,000 times fewer computation resources compared to similar CTM runs. In some instances, this tradeoff proves worthwhile. RCMs’ relative computational efficiency can output air pollution concentrations at much finer spatial resolutions; it also enables consideration of a much larger volume of “what if” scenarios. These considerations are especially important in investigations of the human health impacts of air pollution exposure, where coarse spatial resolution air pollution estimates tend to underpredict pollution exposure, and therefore, health impacts associated with air pollution exposure as well (Paolella et al., 2018; Rieves et al., *in preparation;* Vodonos & Schwartz, 2021). Furthermore, some reduced complexity models still maintain acceptable fidelity with CTM outputs or observed air pollution concentrations (Paolella et al., 2018; Rieves et al., in preparation; Tessum et al., 2017), indicating that these tradeoffs can have little downside in the right application.

This study utilized the Intervention Model for Air Pollution (InMAP), an RCM, to model the annual-average air quality $PM_{2.5}$ and NO_2 concentrations associated with vehicle electrification in Utah. It explored $PM_{2.5}$ and NO_2 because they are directly modeled by—or can be estimated using—InMAP (Tessum et al., 2017) and the relationship between exposure to these pollutants and avoided disease and death onset is robust enough to be considered causal (Forastiere et al., 2024; World Health Organization, 2025). Although RCMs are not as accurate as CTMs, past evaluations have found that InMAP meets modeling performance criteria (MFB <= +/- 60%, MFE <= +/- 75% (Boylan & Russell, 2006) compared to CTM outputs and observed $PM_{2.5}$ concentrations (Paolella et al., 2018; Rieves et al., in preparation; Tessum et al., 2017). Using InMAP instead of a CTM allowed us to consider the health impacts of $PM_{2.5}$ and NO_2 exposure across a uniform 1x1 km output resolution across the entire modeling domain (the state of Utah) for six different combinations of electric vehicle penetration (0%, 60%, 100%) and simulated power systems (additional EV load met by 0%, 40%, and 80% renewable energy) for 2025, 2035, and 2045; running these 18 scenarios at this extent and spatial resolution would have been much more computationally intensive and time consuming with a CTM.

1.3.2 Configuring InMAP

InMAP utilizes input NO_x, SO_x, NH_3, VOC, and primary $PM_{2.5}$ emissions to estimate $PM_{2.5}$ concentrations. Chemical reactions between these gas-phase pollutants create particulate nitrate (pNO_3), particulate sulfate (pSO_4), particulate ammonia (pNH_4) and secondary organic aerosol (SOA), which—in combination with primary $PM_{2.5}$ pollution—form $PM_{2.5}$. InMAP also outputs NO_x concentrations, which are a mixture of nitric oxide (NO), nitrogen dioxide (NO_2), and nitrous oxide (N_2O). The ratio of NO_x:NO_2 can be applied to NO_x concentrations to estimate the NO_2 concentrations.

We configured our model runs with emissions inventories containing the aforementioned pollutants along with emissions release data (temperature, velocity, stack height, stack diameter) for all elevated emissions sources, like power plants. We use fine spatial resolution emissions inputs: onroad emissions have a spatial resolution of 1x1 km, and power plant emissions are represented by a single spatial point. We configured InMAP to output air pollution concentrations to a uniform 1x1 km grid covering the extent of our model domain, Utah.

Fine spatial resolution input emissions and output air pollution concentrations are optimal because they reflect the subtle variations in emissions and air pollution that would otherwise be "averaged out" over space; all spatial data is sensitive to the boundaries it's aggregated within (Jerrett et al., 2010), but using finer scale data reduces the smoothing effect of coarser spatial data. Past evaluations have found that running InMAP with fine spatial resolution input emissions inventories and output air pollution concentrations yields the best model performance, whereas coarse resolution input data and output resolution systematically underpredict air pollution concentrations (Rieves et al., in preparation).

We initialized our model runs with preprocessed WRF-Chem data from 2005, the InMAP default, to represent underlying meteorological conditions (Tessum et al., 2017). Despite the temporal mismatch between meteorological and emissions data, past evaluations found that InMAP outputs for the years 1995 to 2017 that used 2005 meteorology data all met model performance criteria (Tessum et al., 2019). A more recent study using 2019 emissions and 2005 meteorology also found that InMAP met model performance criteria (MFB <= +/- 60%, MFE <= +/- 75%) outlined by Boylan and Russell (2006) for the Wasatch Front, and was within of the MFB threshold by 0.2% for the entire state of Utah; once InMAP outputs were statistically corrected using fused satellite-CTM data, model performance met model performance goal criteria (MFB <= +/- 30%, MFE <= +/- 50%) for both the Utah and Wasatch Front modeling domains (Rieves et al., in preparation).

1.3.3 Estimating NO_2 Concentrations Based on Modeled NO_x

InMAP does not directly estimate NO_2 concentrations. To determine population exposure to NO_2 from InMAP-derived NO_x concentrations we used GEOS-CF data products to calculate the ratio of NO_2 to NO_x concentrations in each grid cell over Utah. The GEOS-CF data, generated by the NASA Center for Climate Simulations (NCCS), utilizes satellite NO_2 column data from the Ozone Monitoring Instrument (OMI) to assimilate NO_2 concentrations in the GEOS-Chem chemical transport model (Keller et al., 2021). Previous works and reports have utilized GEOS-CF products in a wide variety of applications, highlighting its ubiquity as a tool for retrieving hourly pollutant concentrations globally (Amos et al., 2023; Malings et al., 2020). Their hindcast product provides hourly surface NO_2 and NO concentrations at a 0.25° × 0.25° horizontal resolution (roughly 25 × 25 km) globally, which we averaged over all of 2025 and calculated the ratio of NO_2 to NO_x in each grid cell i (χ_i) according to Equation 8:

$$\chi_i = \frac{C_{i,NO_2}}{C_{i,NO_2} + C_{i,NO}} \tag{8}$$

where C_i is the annual-average 2025 surface NO_2 or NO concentration in grid cell i. These ratios were then applied to the NO_x concentrations derived from InMAP that correspond to the same grid cell locations. Because the GEOS-CF data products are at a coarser spatial resolution, we applied the same NO_2:NO_x ratio to all 1x1km grid cells in the InMAP NO_x concentration outputs within the larger GEOS-CF-resolution grid cell. This is justified by the fact that where NO_2 and NO_x concentrations may have significant spatial variability, χ_i does not vary significantly between grid cells (in Utah, the mean of χ_i is 0.87 and its standard deviation is 0.01). Because NO_2 photodissociation is the main chemical mechanism dictating how much NO_2 breaks down into NO, χ_i is primarily dependent on a region's meteorology at our spatiotemporal resolution (Meier et al., 2024). The annual-average available photolytic energy over a single state like Utah does not exhibit significant spatial variability, thus χ_i does not vary significantly. O_3 and VOC concentrations do impact χ_i, but the coarse InMAP model resolution and annual timeframe do not resolve these sub-grid cell phenomena (Meier et al., 2024; Richmond-Bryant et al., 2017).

1.3.4 Correcting Modeled Air Pollution Concentrations

All air pollution models produce statistically biased results, skewed in some direction based on how the model simplifies complex atmospheric dynamics. Applying statistical correction algorithms to CTM or RCM outputs can reduce this bias and increase model concordance with satellite or ground-level monitor data, which is considered the "truth," or more accurately, our best estimation of it (Anenberg et al., 2016; Crooks & Özkaynak, 2014; Diao et al., 2019; Gallagher et al., 2023; Jackson et al., 2023; Jiang & Yoo, 2018). InMAP has a tendency to underpredict $PM_{2.5}$ concentrations, and pSO_4 in particular (Gallagher et al., 2023; Paolella et al., 2018; Rieves et al., in preparation; Tessum et al., 2017). Studies have implemented correction algorithms to adjust InMAP-output component pollutants of PM2.5 based on in situ monitoring data or satellite data, finding that these approaches can improve InMAP performance, especially for pSO_4 (Gallagher et al., 2023; Jackson et al., 2023). Because certain sectors—including electricity generation—are responsible for the bulk of pSO_4 emissions, statistically correcting InMAP outputs can help characterize more accurately each sector's contribution to overall $PM_{2.5}$ concentrations.

We applied state-specific statistical correction factors for Utah published in Gallagher et al. (2023) (Table 2) to correct $PM_{2.5}$ component emissions (pNO_3, pSO_4, and pNH_4). These were calculated using the ratio between InMAP-predicted $PM_{2.5}$ component concentrations and Washington University North American Regional Estimates annual average satellite concentrations for pSO_4, pNO_3, and pNH_4. They do not provide correction factors for primary $PM_{2.5}$ or SOA, likely because satellite data is not available for these pollutants. We did not apply correction factors to NO_2 concentrations because no published scaling factors derived from InMAP outputs are available. Additional details on how scaling factors were created can be found in Gallagher et al. (2023).

Table 2: Utah-specific InMAP scaling factors for $PM_{2.5}$ components

pNO_3	pSO_4	pNH_4
4.43	16.33	0.70

We used Equation 9 to calculate total corrected $PM_{2.5}$ for each 1x1km grid cell:

$$\begin{aligned} &\text{Corrected } PM_{2.5,i} = \\ &\left(4.43 \times pNO_{3,i}\right) + \left(16.33 \times pSO_{4,i}\right) \\ &+\left(0.7 \times pNH_{4,i}\right) + \text{Primary } PM_{2.5,i} + SOA_i \end{aligned} \tag{9}$$

where i represents each grid cell.

1.3.5 Calculating Differences in Air Pollution Concentrations for Each Scenario Run

We calculated the differences in $PM_{2.5}$ and NO_2 associated with the combination of onroad and power-sector emissions changes associated with each vehicle electrification scenario in each 1x1km grid cell using Equation 10 and Equation 11:

$$\Delta PM_{2.5,(t,i)} = \left(v_{0,(t,i)} - v_{(t,i)}\right) + \left(p_{0,(t,i)} - p_{(t,i)}\right) \tag{10}$$

$$\Delta NO_{2,(t,i)} = \left(v_{0,(t,i)} - v_{(t,i)}\right) + \left(p_{0,(t,i)} - p_{(t,i)}\right) \tag{11}$$

where $v_{0_{(t,i)}}$ represents baseline onroad concentrations of $PM_{2.5}$ (Equation 10) or NO_2 (Equation 11) for grid cell i and scenario year t, $v_{(t,i)}$ represents scenario onroad concentrations of $PM_{2.5}$ (Equation 10) or NO_2 (Equation 11) for grid cell i and scenario year t, $p_{0_{(t,i)}}$ represents baseline power sector concentrations of $PM_{2.5}$ (Equation 10) or NO_2 (Equation 11) for grid cell i and scenario year t, and $p_{(t,i)}$ represents scenario power sector concentrations of $PM_{2.5}$ (Equation 10) or NO_2 (Equation 11) for grid cell i and scenario year t.

In our calculations, we kept the scenario year consistent (e.g. the scenario and baseline concentrations are from the same year) to account for projected increases in onroad emissions in future scenario years. Based on the setup of Equation 10 and Equation 11, positive values indicate a *decrease* in air pollution concentrations associated with the scenario, whereas negative values indicate an *increase*.

After calculating the change in $PM_{2.5}$ and NO_2 concentrations associated with each scenario for each grid cell, we spatially aggregated air pollution concentrations to the Census tract, the unit of our health impact analysis.

1.4 Health Impact Analysis

Conducting a spatial health impact analysis (HIA) of air pollution exposure requires multiple data inputs: (1) air pollution concentration data, (2) population data, (3) baseline morbidity or mortality data (incidence data) depending on the health impact being modeled, and (4) a concentration response function (CRF) that quantifies the relationship between long-term pollution exposure and each health outcome.

We used air pollution data described in the section above for $PM_{2.5}$ and NO_2 concentrations. We used projected, age-stratified population data (described above) at the Census tract level for each scenario year we modeled (2025, 2035, 2045). For underlying mortality incidence data, we used the 2024 CDC WONDER county-level death rates as our underlying mortality data (Center for Disease Control and Prevention, 2024) because death rates for 2025 have not yet been released. We assigned county-level incidence rates to all Census tracts within the county. For underlying morbidity incidence, we used age-stratified 2023 Global Burden of Disease (GBD) data for the state of Utah (Insitute for Health Metrics and Evaluation, 2025); no finer spatial resolution incidence variables were available for these analyses and 2023 is the most recent year of data in this dataset.

We used linear concentration response functions (CRFs) to estimate the relationship between $PM_{2.5}$ and NO_2, and each of the health endpoints we considered: all-cause mortality and the onset dementia, stroke, lung cancer, ischemic heart disease events, COPD, asthma, Type 2 diabetes, COPD, Autism Spectrum Disorders (ASD), and acute lower respiratory infections (ALRI). These CRFs are published as part of the World Health Organization's (WHO) recently published guidance from the Health Risks of Pollution in Europe (HRAPIE-2) project (World Health Organization, 2025). The HRAPIE project estimates CRFs for all these conditions by conducting a meta-analysis of previously published studies for each pollutant-health outcome pair. Their meta-analysis utilizes stringent inclusion criteria regarding causality, the number of studies included in selected meta-analyses, statistical significance and confidence intervals, geographical coverage—to ensure that results are globally applicable rather than tied to a specific geography—weight distribution of the meta-analytic weights, and the consistency of results (Forastiere et al., 2024; World Health Organization, 2025). Furthermore, these CRFs are not geographically specific and are suitable for application in areas with low annual average $PM_{2.5}$ and NO_2 pollution (Forastiere et al., 2024; World Health Organization, 2025), including Utah. Because all morbidity CRFs are applicable to specific age ranges but these age ranges do not necessarily match the incidence rate or age-stratified population data, we use the closest interval. We provide a summary of incidence data and the relative risk for each pollutant-health outcome pair in the supplement **(Appendix 1)**.

We calculate the hypothetical number of deaths or avoided disease onset attributable to the modeled change in $PM_{2.5}$ or NO_2 concentration for each vehicle electrification scenario using Equation 12:

$$\sum_i \Delta y_i = y_{0,i} p_i \left(1 - e^{-\beta \Delta x_i}\right) \quad (12)$$

Where Δy is the change in morbidity or mortality for Census tract i, $y_{(0)_i}$ is the baseline mortality or incidence rate for Census tract i, p_i is the population for Census tract i, β is the natural log of the relative risk (RR) from the CRF divided by the per unit change in the pollutant (e.g., 10 ug/m^3), and Δx_i is the observed change in $PM_{2.5}$ or NO_2 concentrations between the baseline and electrification scenarios for Census tract i. For morbidity calculations, the $y_{(0)_i}$ term is replaced with y_0 because the underlying incidence rates do not vary spatially and are the same across the state.

We calculated our "best estimate" of the avoided morbidity and mortality associated with each scenario using the point estimate for the RR and CRF. Due to the significant uncertainty associated with conducting health impact assessments (HIAs), we also calculate "uncertainty intervals"—the lower and upper bounds of our estimate—calculated using the low estimates for the RR and CRF ("low-low") and the high estimates for the RR and CRF ("high-high"). We are unable to quantify the uncertainty of simulated air pollution concentrations or projected population data, so these are not accounted for in our uncertainty intervals.

We completed air quality modeling pre- and post-processing, as well as all spatial data analysis in Python 3.10 (Python, 2021) on the CU Research Computing (CURC) Alpine supercomputing nodes.

2 Results

All scenarios resulted in net improvements in $PM_{2.5}$ and NO_2 concentrations (Figure 4 –4), indicating that vehicle electrification might reduce $PM_{2.5}$ and NO_2 pollution in Utah provided that vehicle adoption and electricity generation look very similar to the scenarios explored here. Statewide annual average reductions in air pollution concentrations ranged across scenarios from 0.72 to 1.58 μg/m^{-3} for $PM_{2.5}$ and 0.96 to 2.11 μg/m^{-3} for NO_2 depending on the extent of vehicle electrification (60% versus 100%) and the scenario year. The 60% scenarios delivered lower reductions in air pollution concentrations compared to the 100% vehicle electrification scenarios. We observed that reductions in $PM_{2.5}$ and NO_2 increased in future decades due to projected increases in population and onroad emissions in the state. Most of the reductions in $PM_{2.5}$ and NO_2 occurred within the Wasatch Front, which had higher baseline onroad emissions compared to the rest of the state, where average reductions across the Wasatch Front extent ranged from 0.87 to 1.9 μg/m^{-3} reduction in annual average NO_2 concentrations and 1.24 to 2.72 μg/m^{-3} annual average $PM_{2.5}$. Reductions were even higher than these averages in near-highway communities.

We observed that different assumptions about the power sector—for example, whether added load was powered by 0% or 80% renewable energy—had a negligible impact on air pollution concentrations for either $PM_{2.5}$ or NO_2 (Figures 28-31; Appendix Figures 38-41). The increase in electric generation associated with vehicle electrification resulted in very small increases in $PM_{2.5}$ and NO_2 pollution that were offset by much larger reductions in $PM_{2.5}$ and NO_2 concentrations from the decreases in onroad emissions due to vehicle electrification. For example, the 2045 100% vehicle electrification, 0% renewable energy scenario represents the greatest increase in electric load of any scenario we modeled (26 TWh), but the *highest* Census tract-level increases in air pollution concentrations associated with the power sector in this scenario were 0.08 and 0.01 μg/m^{-3} for $PM_{2.5}$ and NO_2, respectively; in contrast, the *average* reductions in air pollution concentrations associated with reductions in onroad emissions for this scenario were much higher: 1.58 and 2.11 μg/m^{-3} , respectively (Figures

28-31; Appendix Figures 38-41). It is worth noting that the scenarios with the highest potential to negatively impact air pollution concentrations—100% vehicle electrification with added load met by 0% renewable energy—assume that a substantial portion of added load associated with vehicle electrification is met by power plants in Wyoming, from 31% (2045) to 41% (2025), and that a majority of the added load met within the state of Utah is met by natural gas plants, from 54% (2025) to 70% (2045) instead of coal-fired power plants (Appendix Table 5). Air pollution concentrations could be higher if a larger proportion of the load were met by coal fired power plants in the state of Utah, although this is not something that we explored in our analyses.

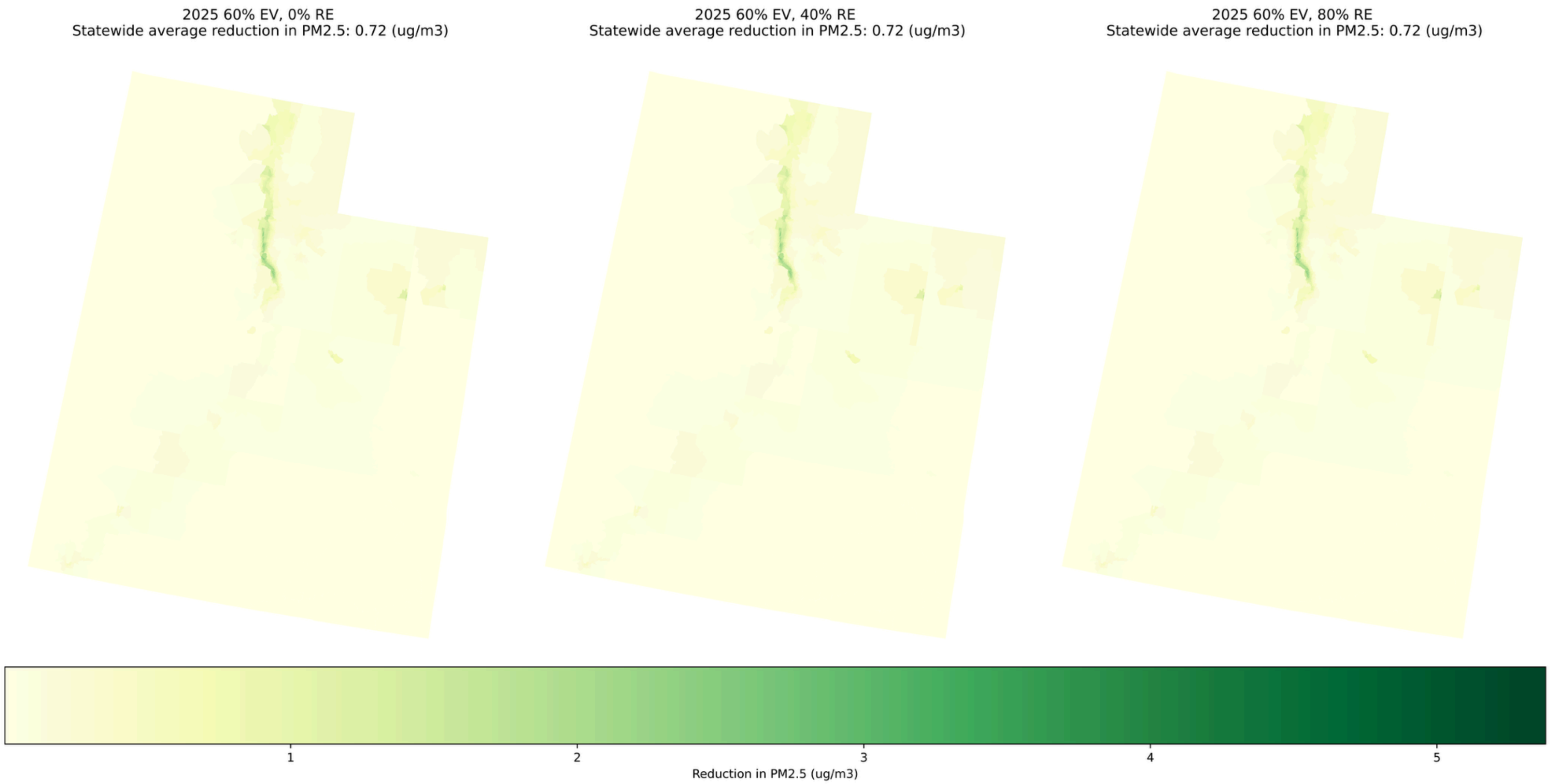

Figure 4: Reductions in $PM_{2.5}$ ($\mu g/m^{-3}$) in Utah associated with 60% vehicle electrification powered by 0%, 40%, and 80% renewable energy (RE), 2025

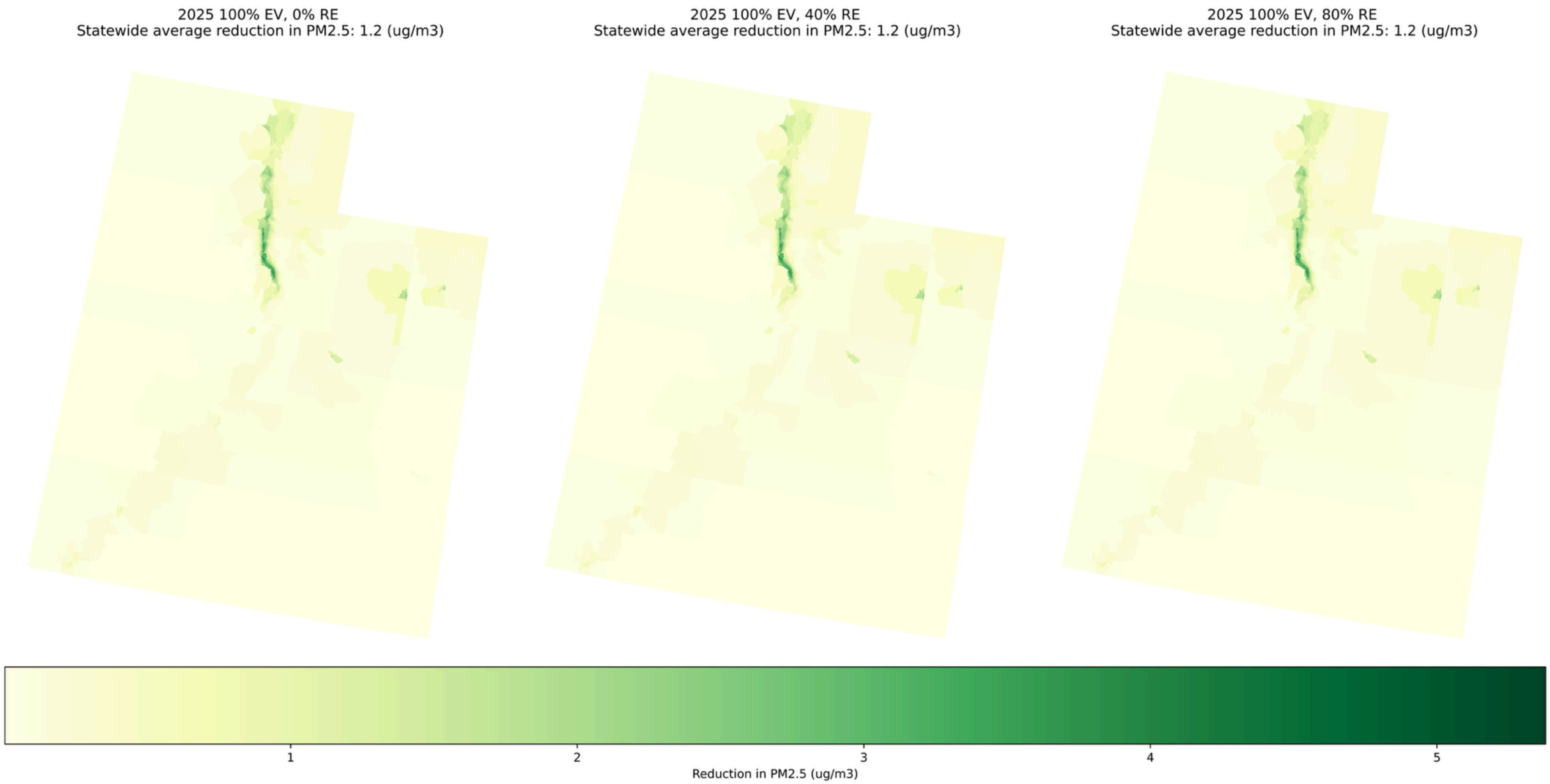

Figure 5: Reductions in $PM_{2.5}$ ($\mu g/m^{-3}$) in Utah associated with 100% vehicle electrification powered by 0%, 40%, and 80% renewable energy (RE), 2025

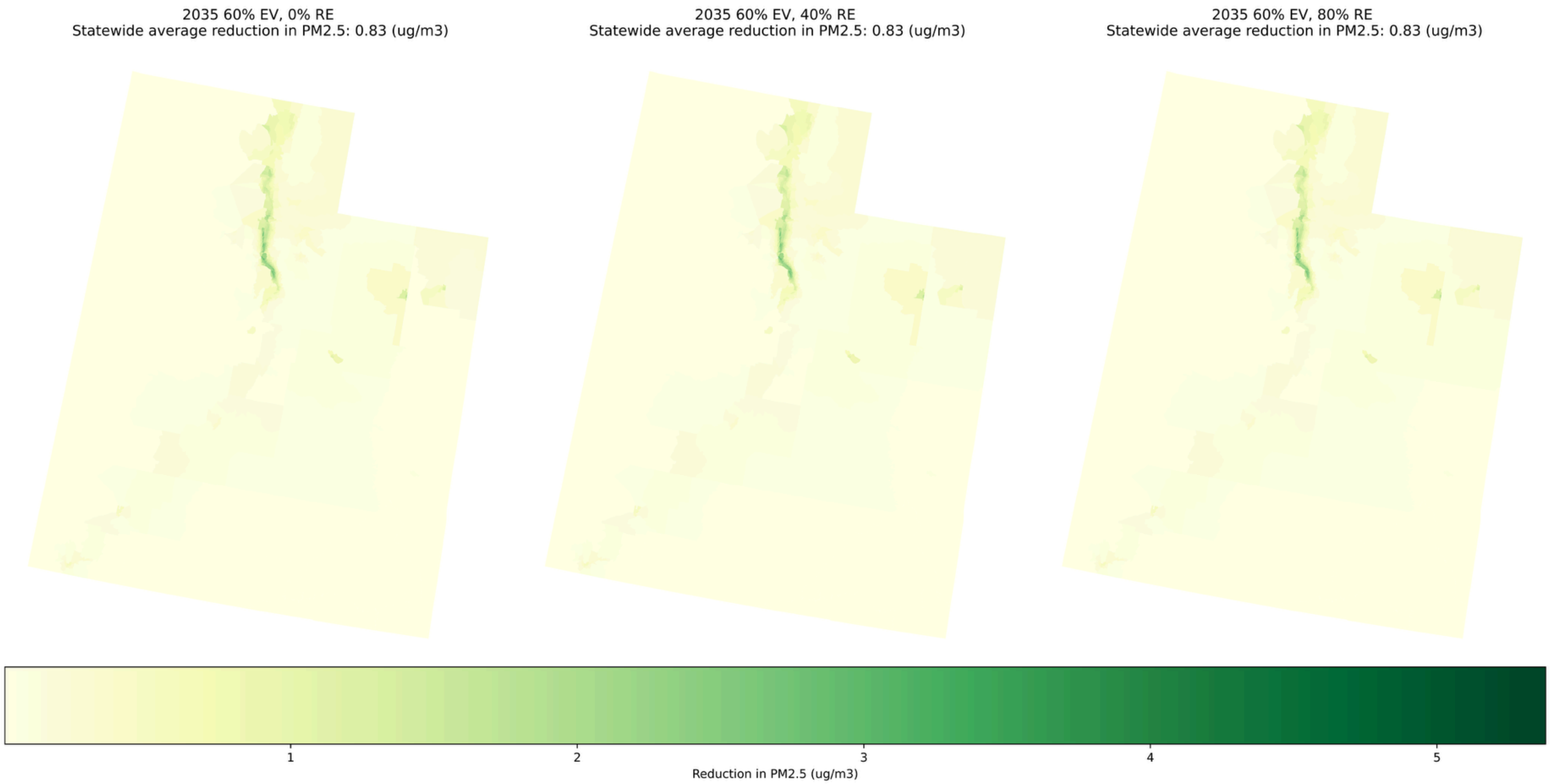

Figure 6: Reductions in $PM_{2.5}$ ($\mu g/m^{-3}$) in Utah associated with 60% vehicle electrification powered by 0%, 40%, and 80% renewable energy (RE), 2035

Figure 7: Reductions in $PM_{2.5}$ ($\mu g/m^{-3}$) in Utah associated with 100% vehicle electrification powered by 0%, 40%, and 80% renewable energy (RE), 2035

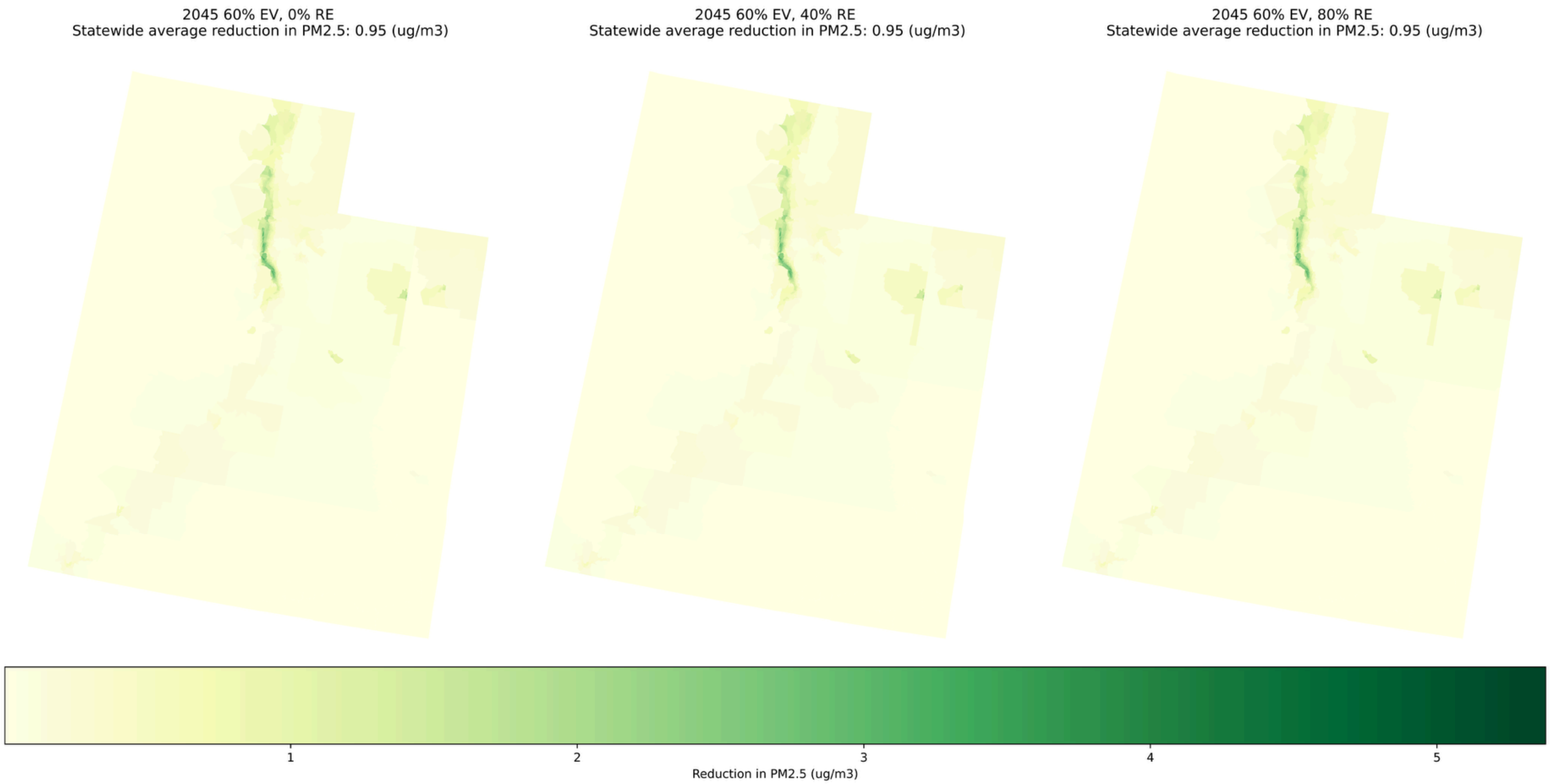

Figure 8: Reductions in $PM_{2.5}$ ($\mu g/m^{-3}$) in Utah associated with 60% vehicle electrification powered by 0%, 40%, and 80% renewable energy (RE), 2045

Figure 9: Reductions in $PM_{2.5}$ ($\mu g/m^{-3}$) in Utah associated with 100% vehicle electrification powered by 0%, 40%, and 80% renewable energy (RE), 2045

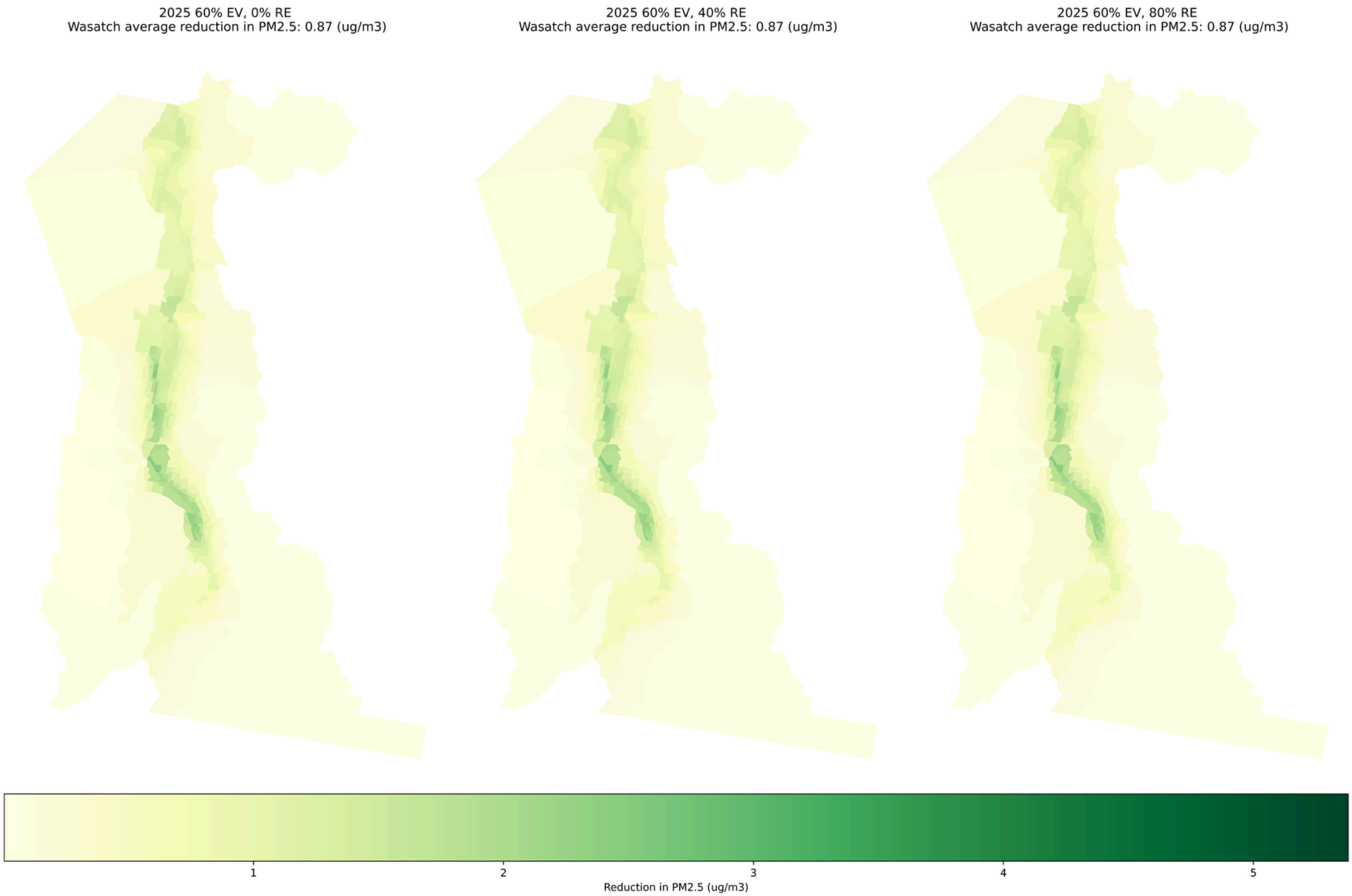

Figure 10: Reductions in $PM_{2.5}$ ($\mu g/m^{-3}$) across the Wasatch Front associated with 60% vehicle electrification powered by 0%, 40%, and 80% renewable energy (RE), 2025

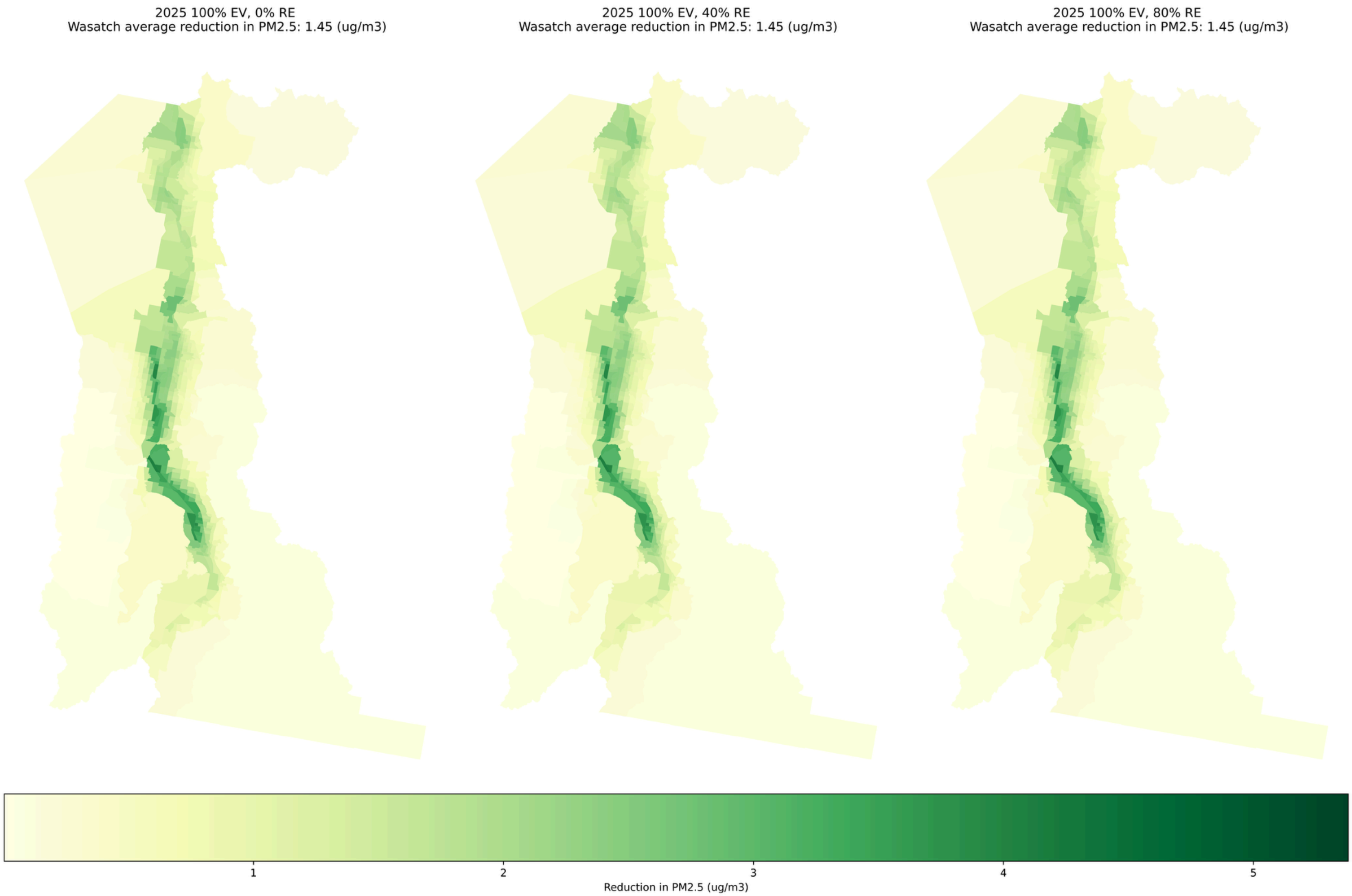

Figure 11: Reductions in $PM_{2.5}$ ($\mu g/m^{-3}$) across the Wasatch Front associated with 100% vehicle electrification powered by 0%, 40%, and 80% renewable energy (RE), 2025

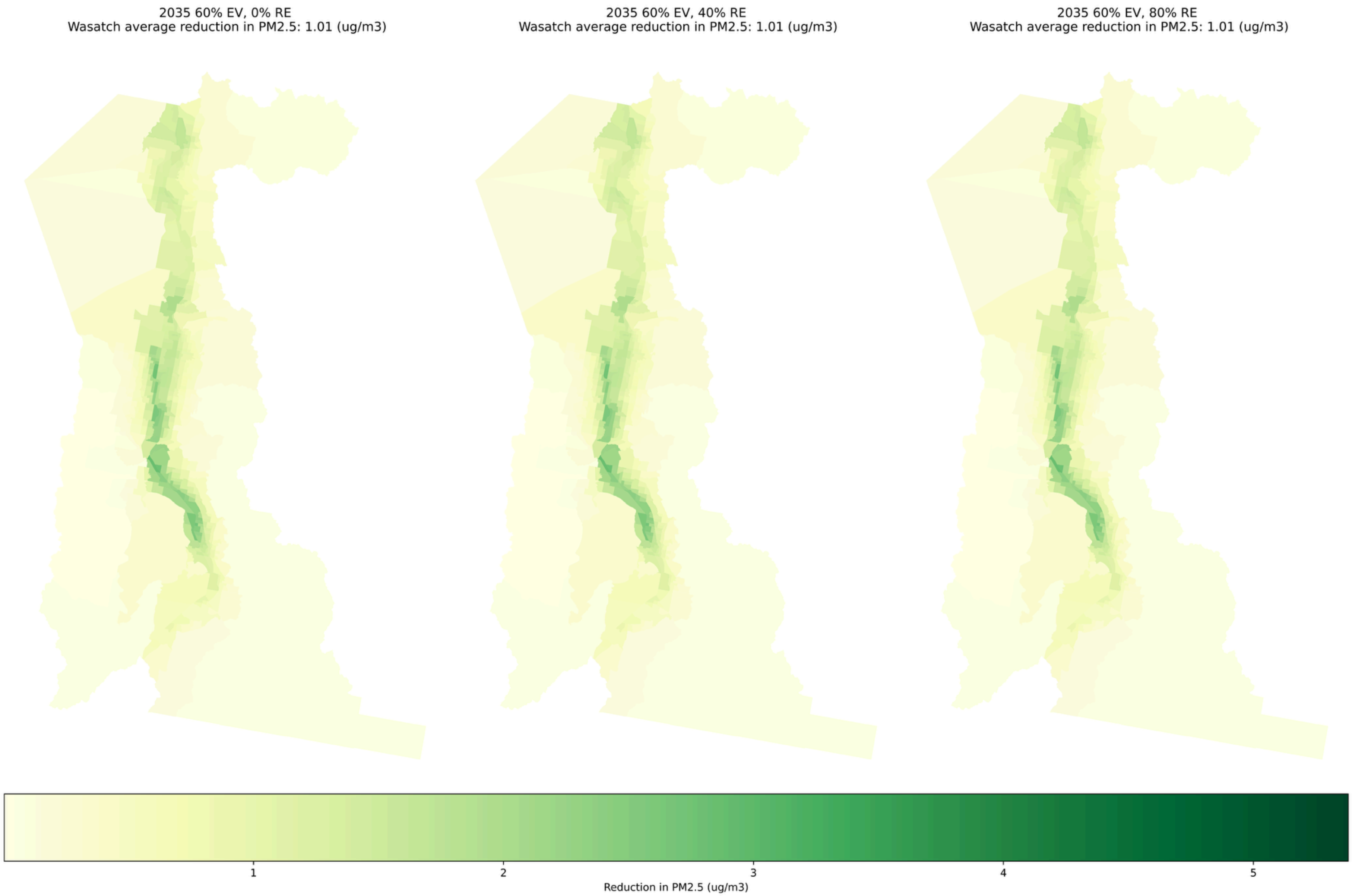

Figure 12: Reductions in $PM_{2.5}$ ($\mu g/m^{-3}$) across the Wasatch Front associated with 60% vehicle electrification powered by 0%, 40%, and 80% renewable energy (RE), 2035

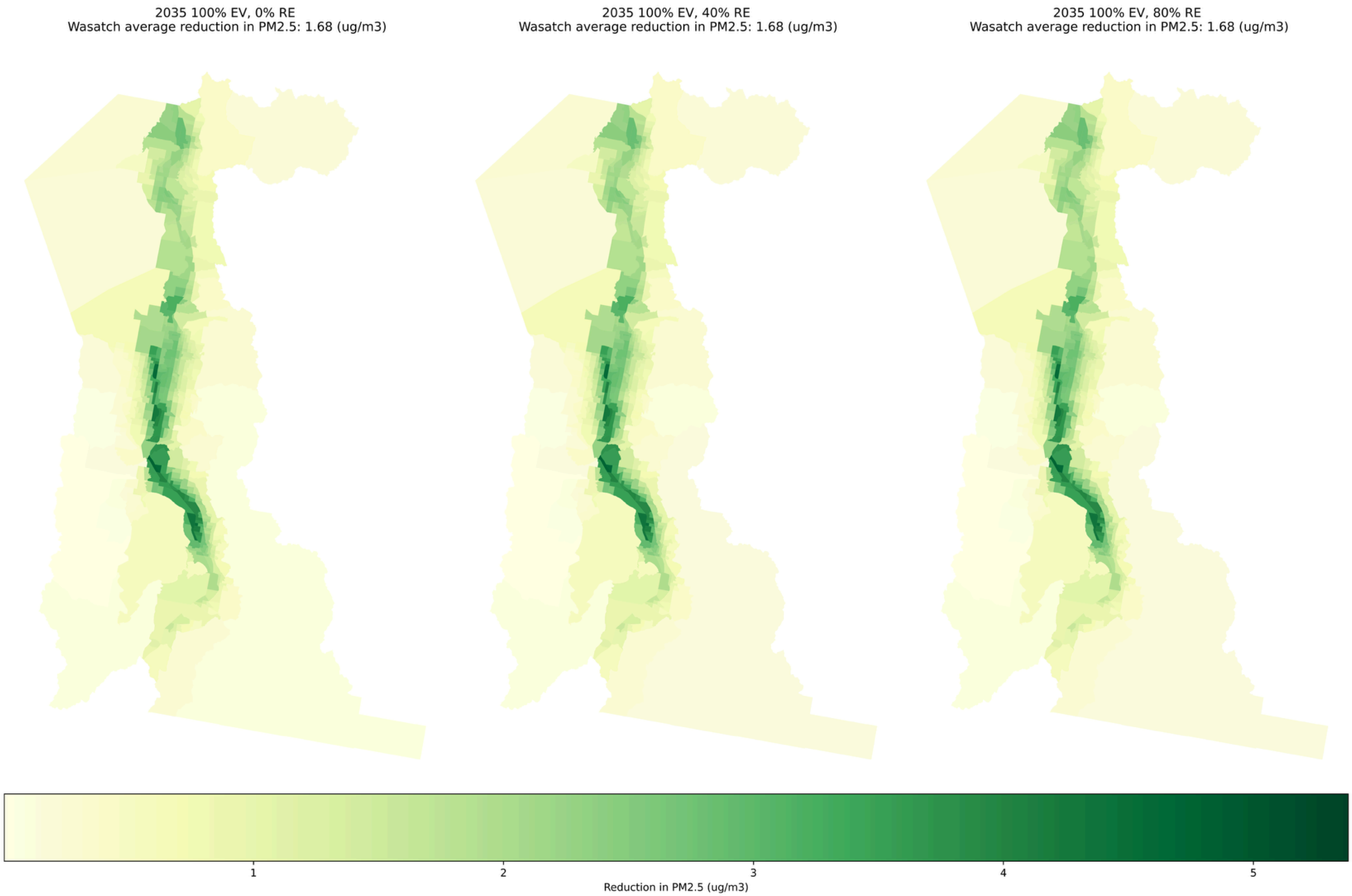

Figure 13: Reductions in $PM_{2.5}$ ($\mu g/m^{-3}$) across the Wasatch Front associated with 100% vehicle electrification powered by 0%, 40%, and 80% renewable energy (RE), 2035

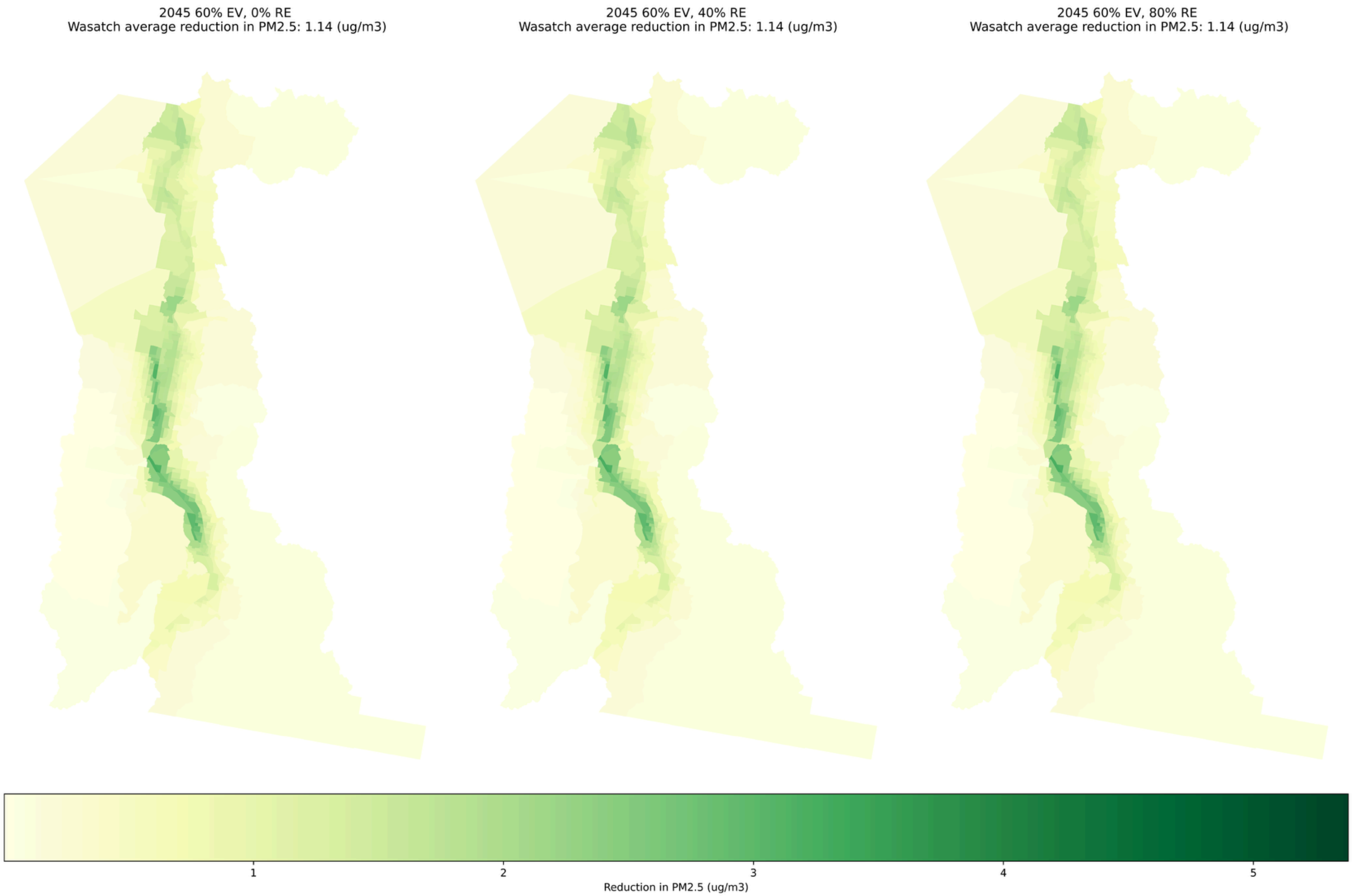

Figure 14: Reductions in $PM_{2.5}$ ($\mu g/m^{-3}$) across the Wasatch Front associated with 60% vehicle electrification powered by 0%, 40%, and 80% renewable energy (RE), 2045

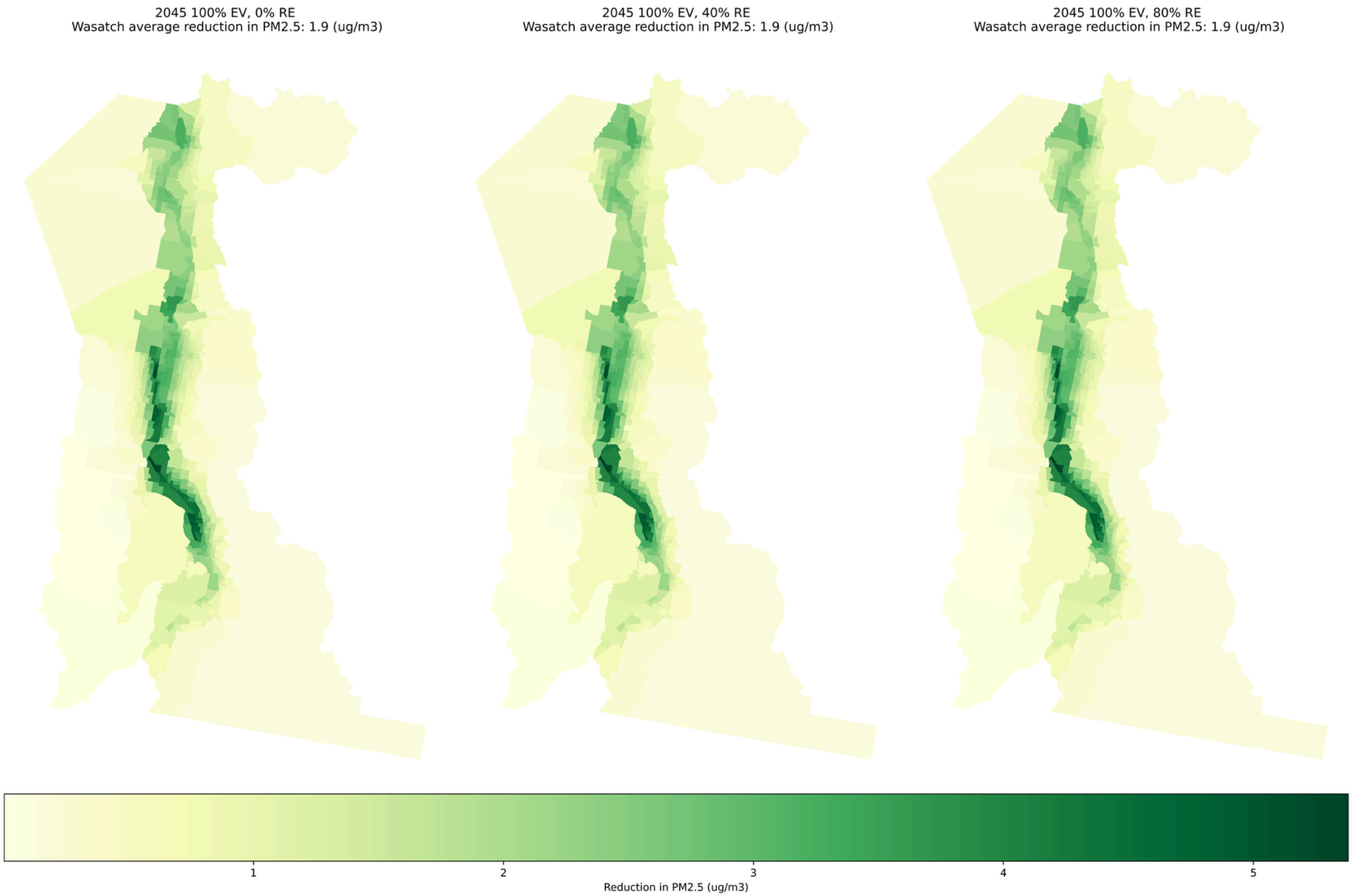

Figure 15: Reductions in $PM_{2.5}$ ($\mu g/m^{-3}$) across the Wasatch Front associated with 100% vehicle electrification powered by 0%, 40%, and 80% renewable energy (RE), 2045

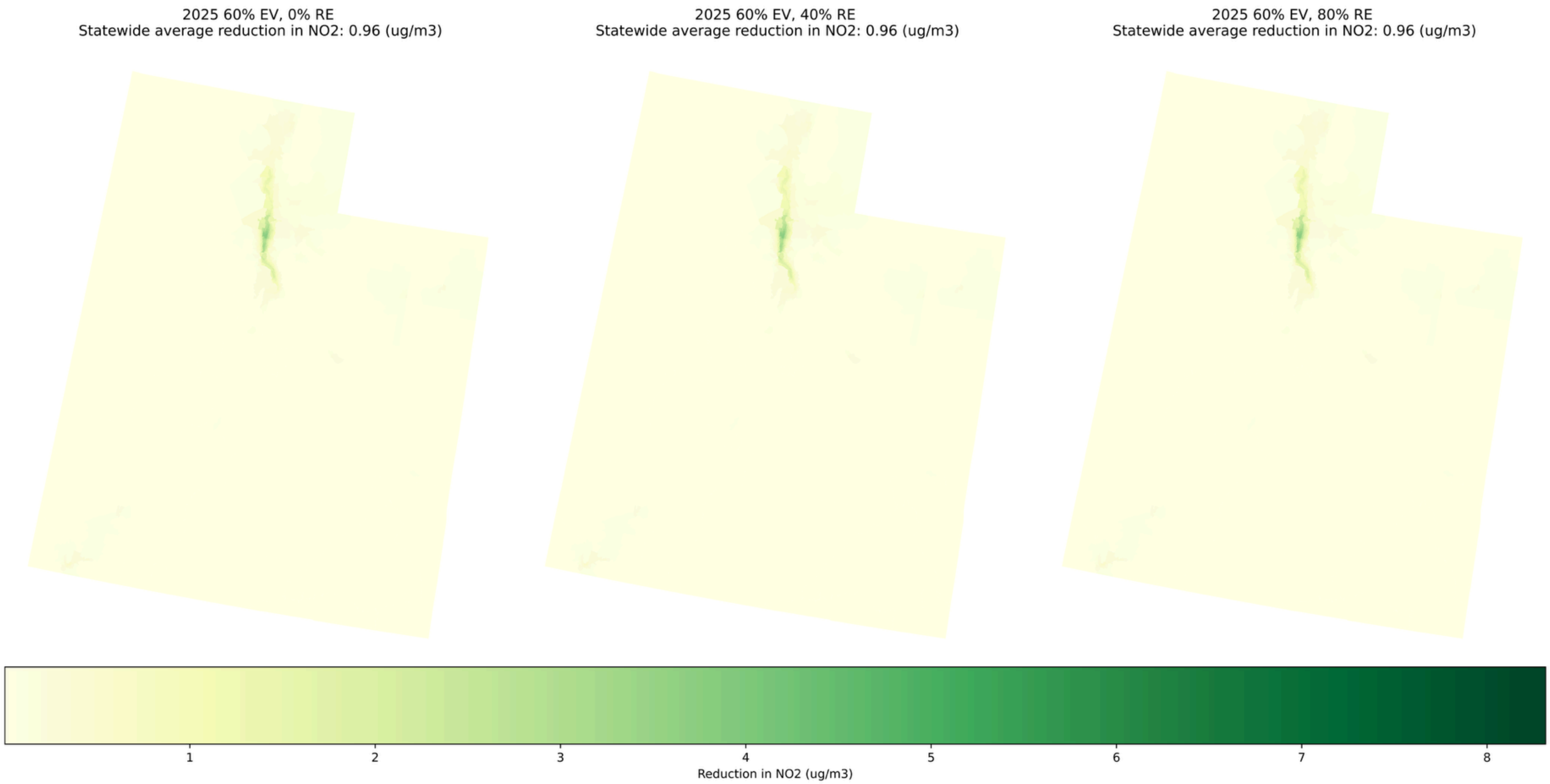

Figure 16: Reductions in NO_2 ($\mu g/m^{-3}$) in Utah associated with 60% vehicle electrification powered by 0%, 40%, and 80% renewable energy (RE), 2025

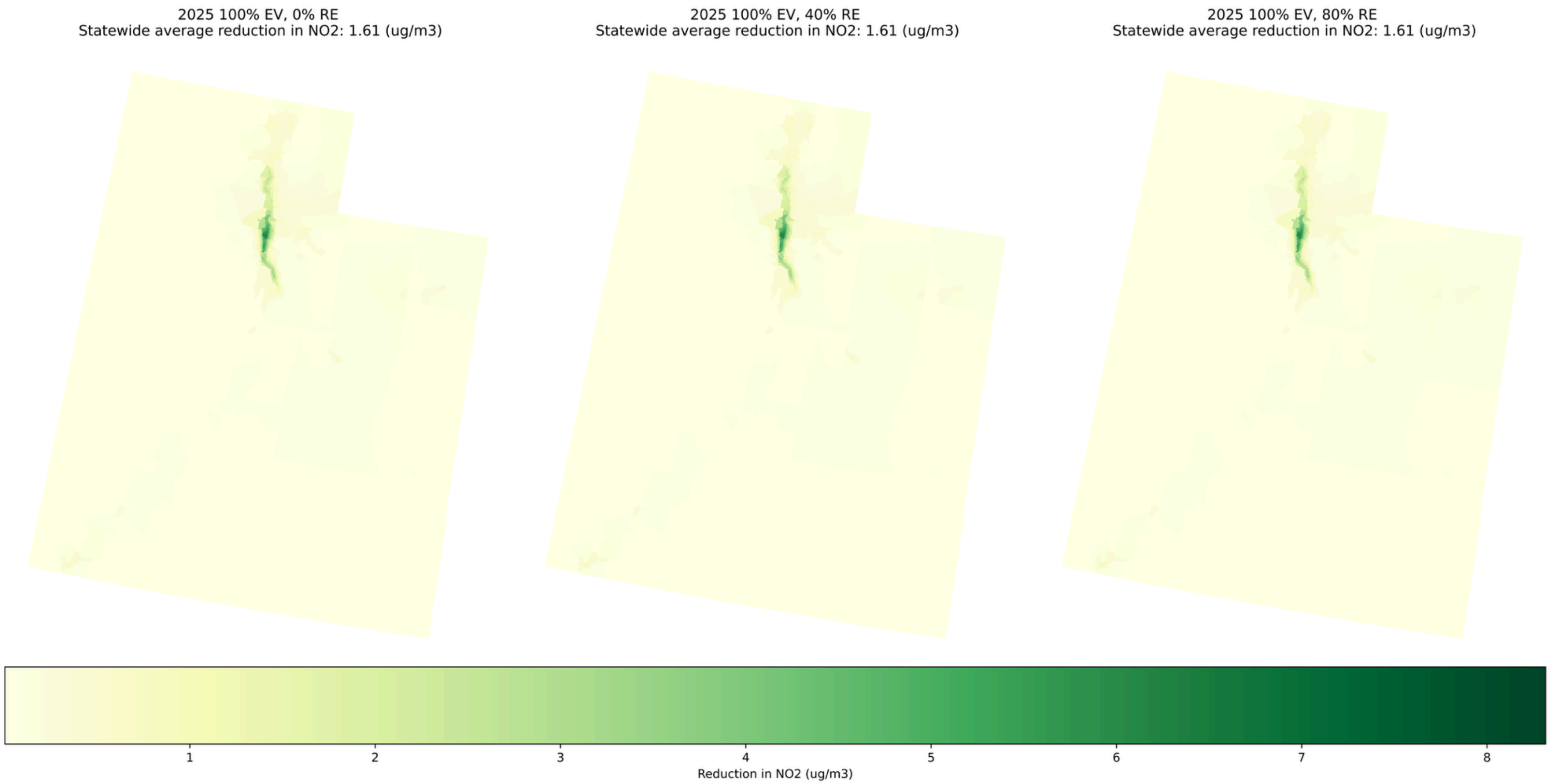

Figure 17: Reductions in NO_2 ($\mu g/m^{-3}$) in Utah associated with 100% vehicle electrification powered by 0%, 40%, and 80% renewable energy (RE), 2025

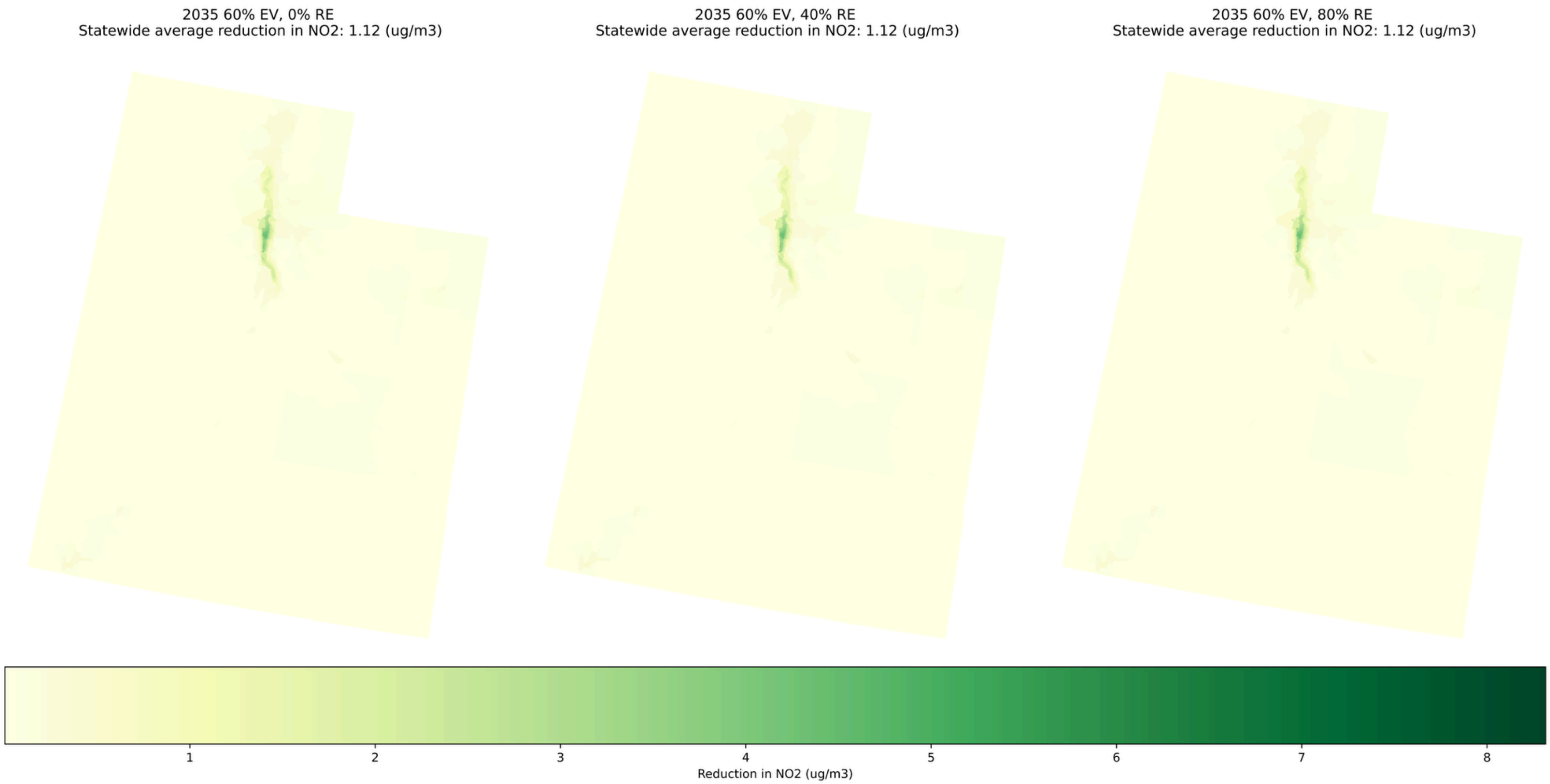

Figure 18: Reductions in NO_2 ($\mu g/m^{-3}$) in Utah associated with 60% vehicle electrification powered by 0%, 40%, and 80% renewable energy (RE), 2035

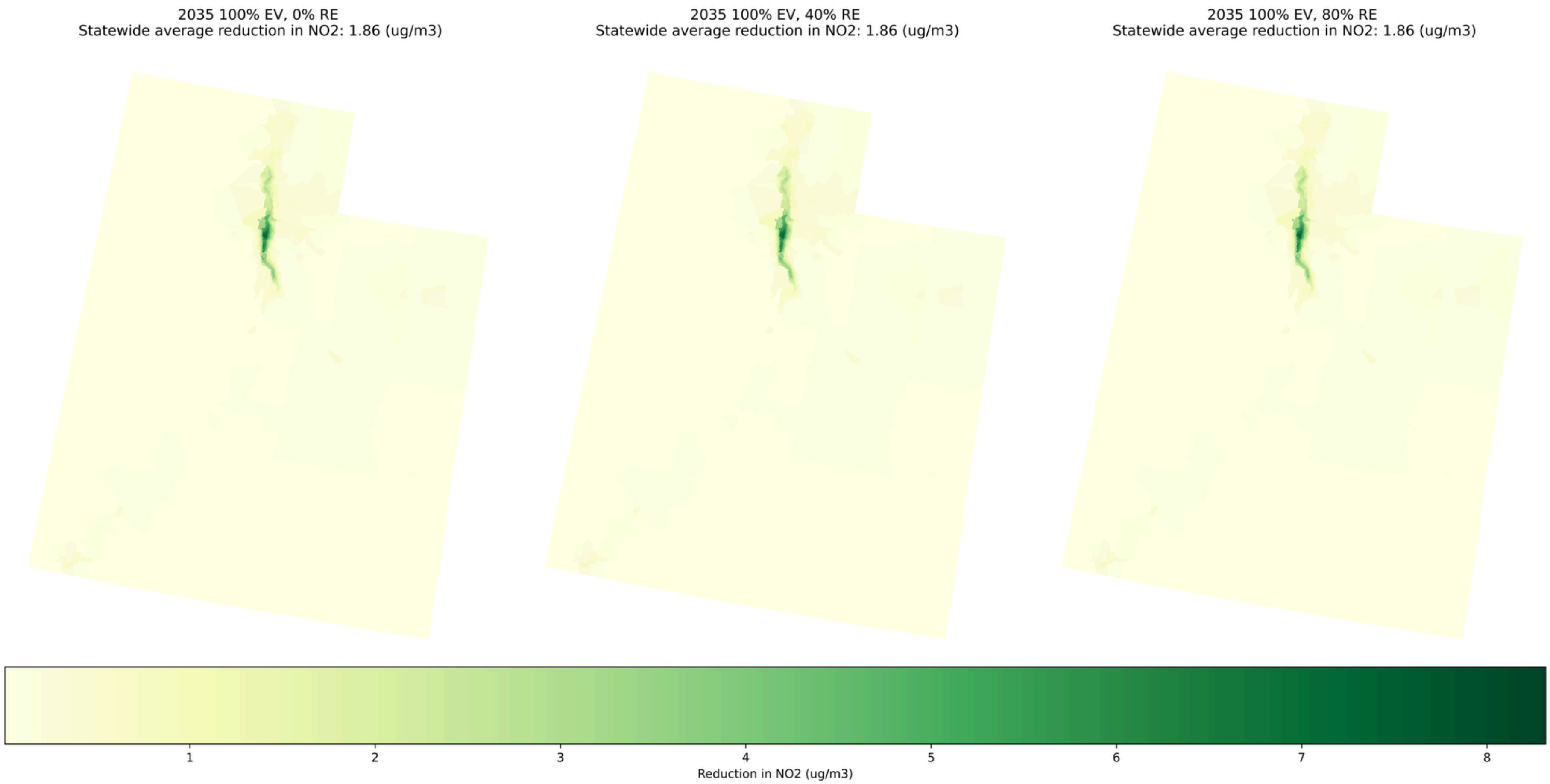

Figure 19: Reductions in NO_2 ($\mu g/m^{-3}$) in Utah associated with 100% vehicle electrification powered by 0%, 40%, and 80% renewable energy (RE), 2035

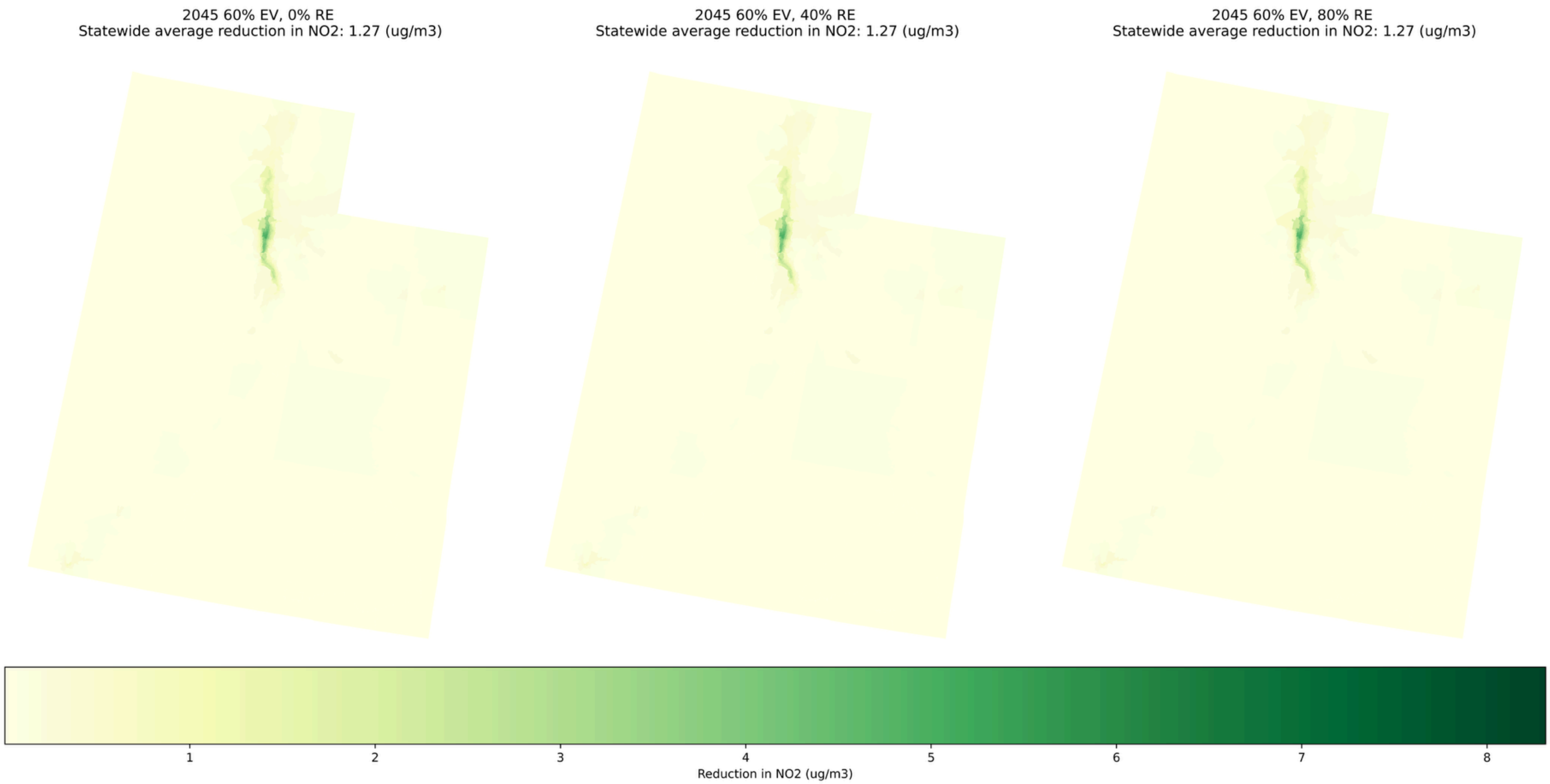

Figure 20: Reductions in NO_2 ($\mu g/m^{-3}$) in Utah associated with 60% vehicle electrification powered by 0%, 40%, and 80% renewable energy (RE), 2045

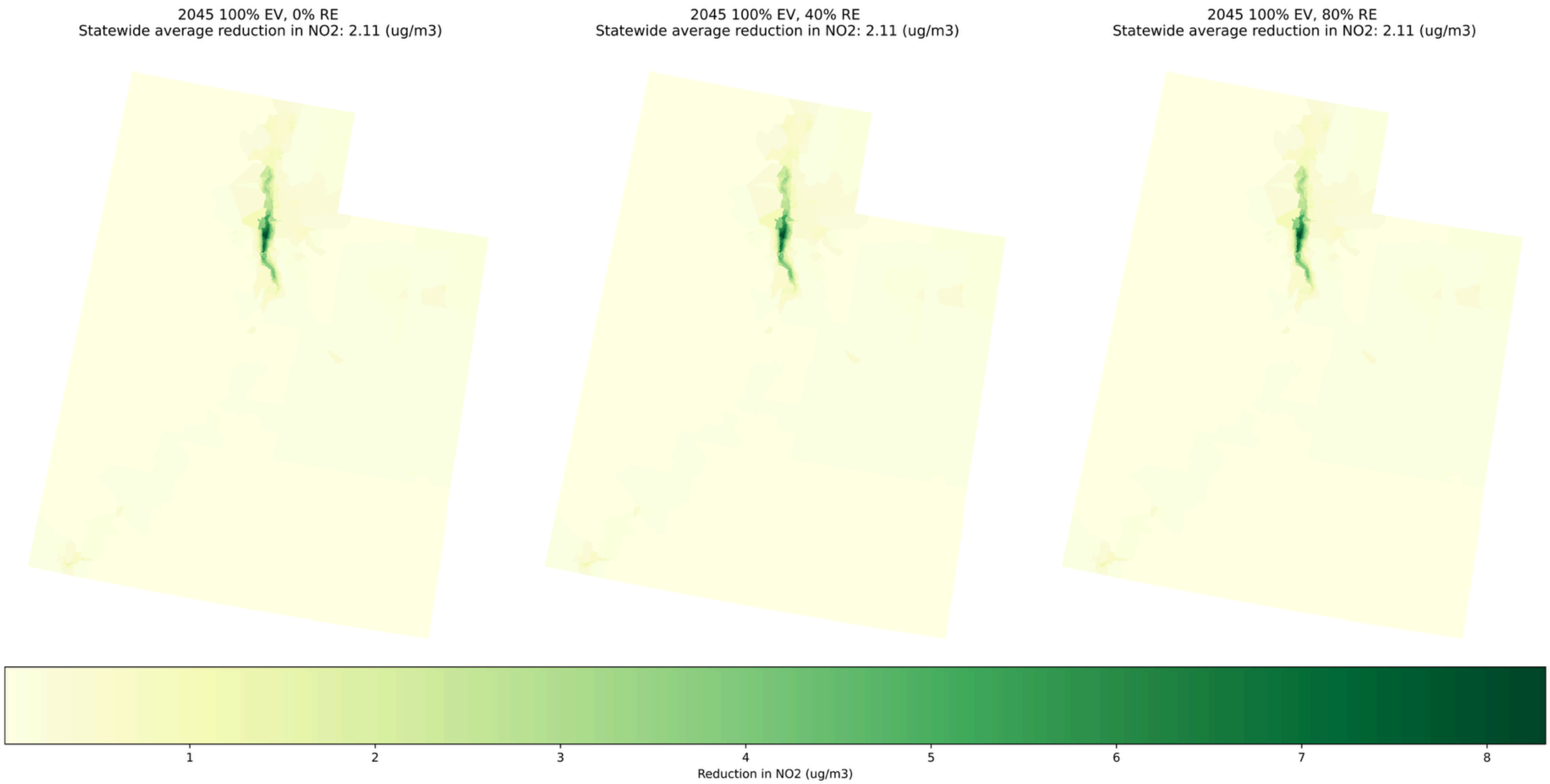

Figure 21: Reductions in NO_2 ($\mu g/m^{-3}$) in Utah associated with 100% vehicle electrification powered by 0%, 40%, and 80% renewable energy (RE), 2045

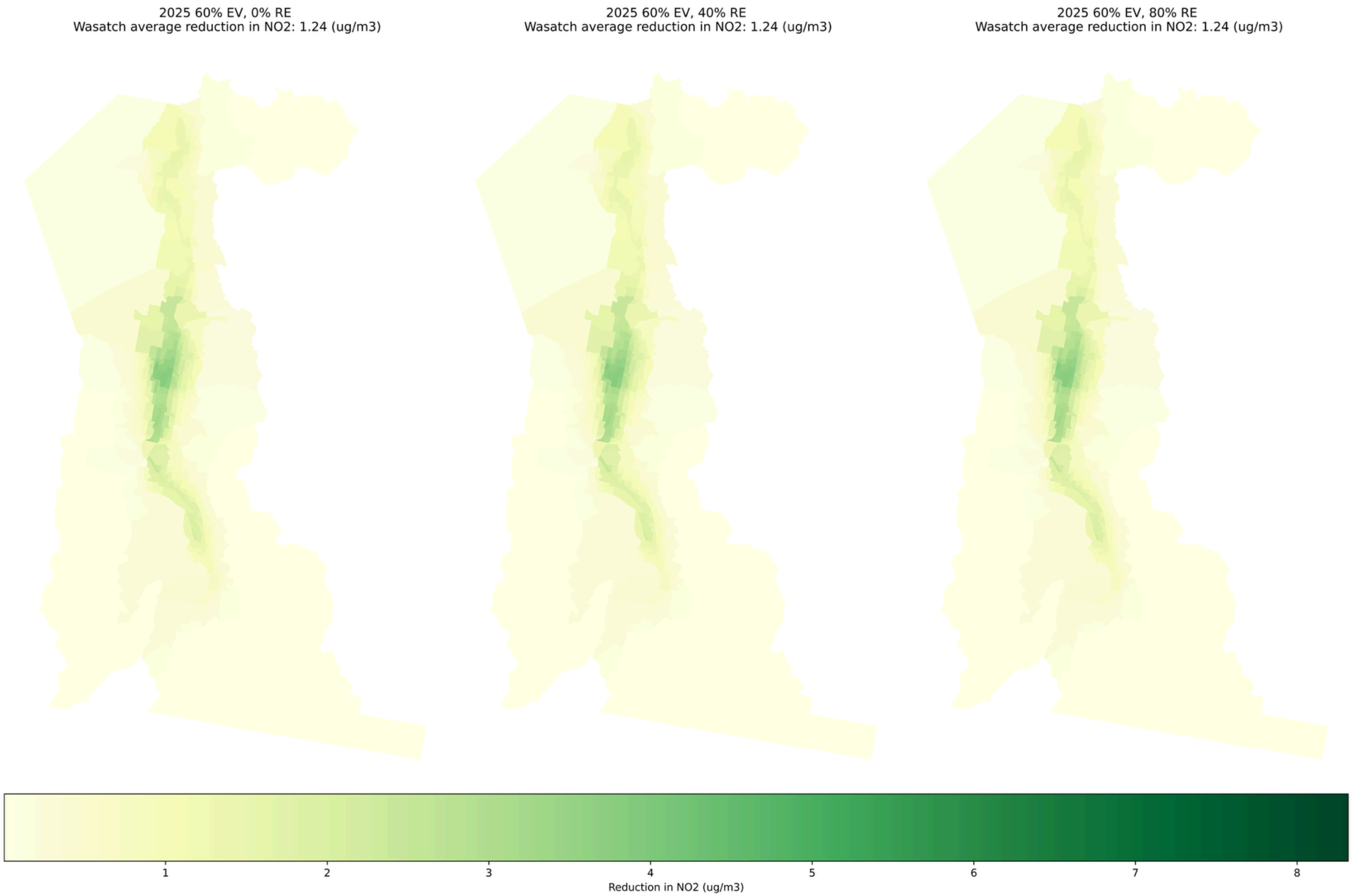

Figure 22: Reductions in NO_2 ($\mu g/m^{-3}$) across the Wasatch Front associated with 60% vehicle electrification powered by 0%, 40%, and 80% renewable energy (RE), 2025

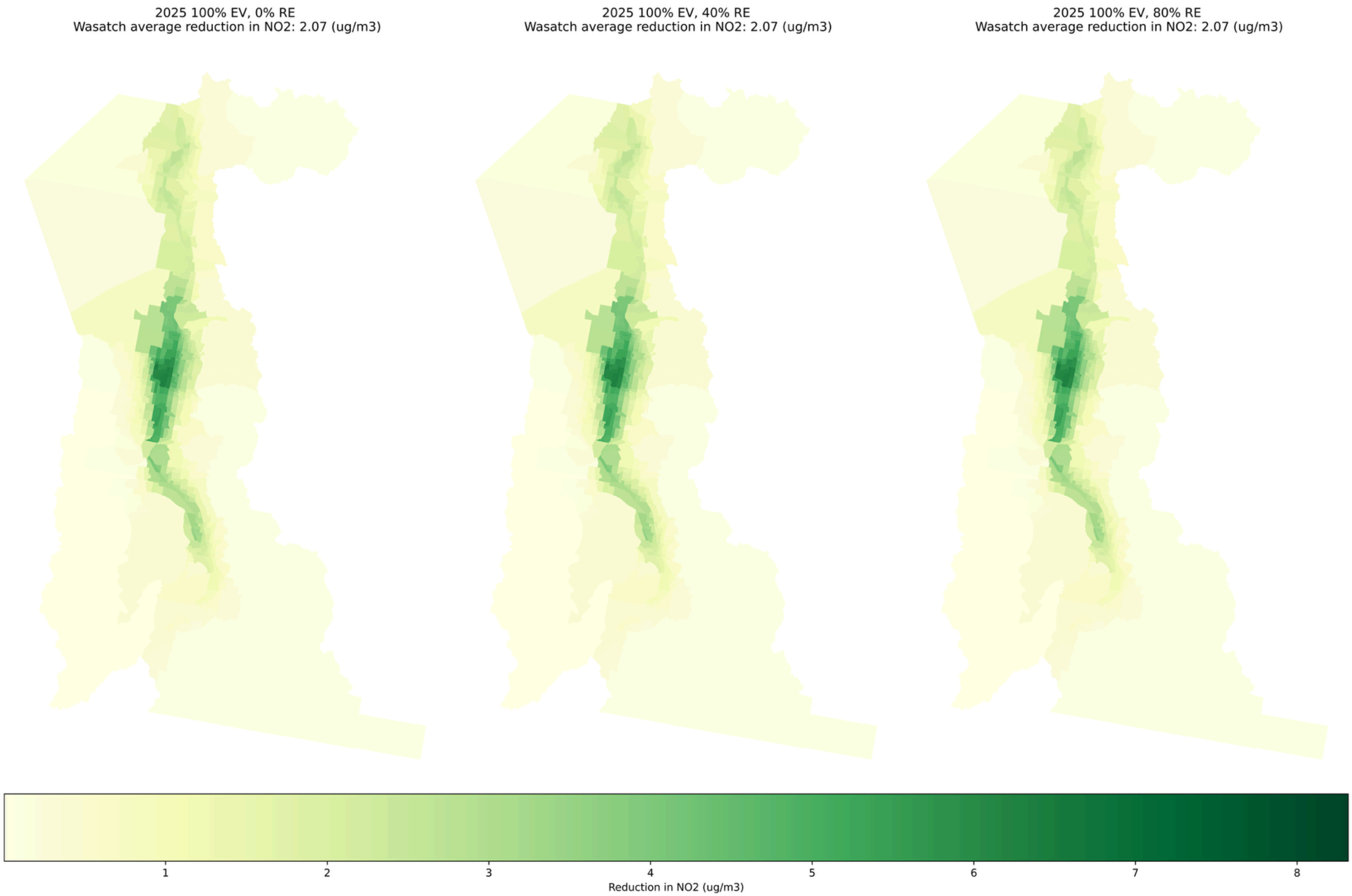

Figure 23: Reductions in NO_2 ($\mu g/m^{-3}$) across the Wasatch Front associated with 100% vehicle electrification powered by 0%, 40%, and 80% renewable energy (RE), 2025

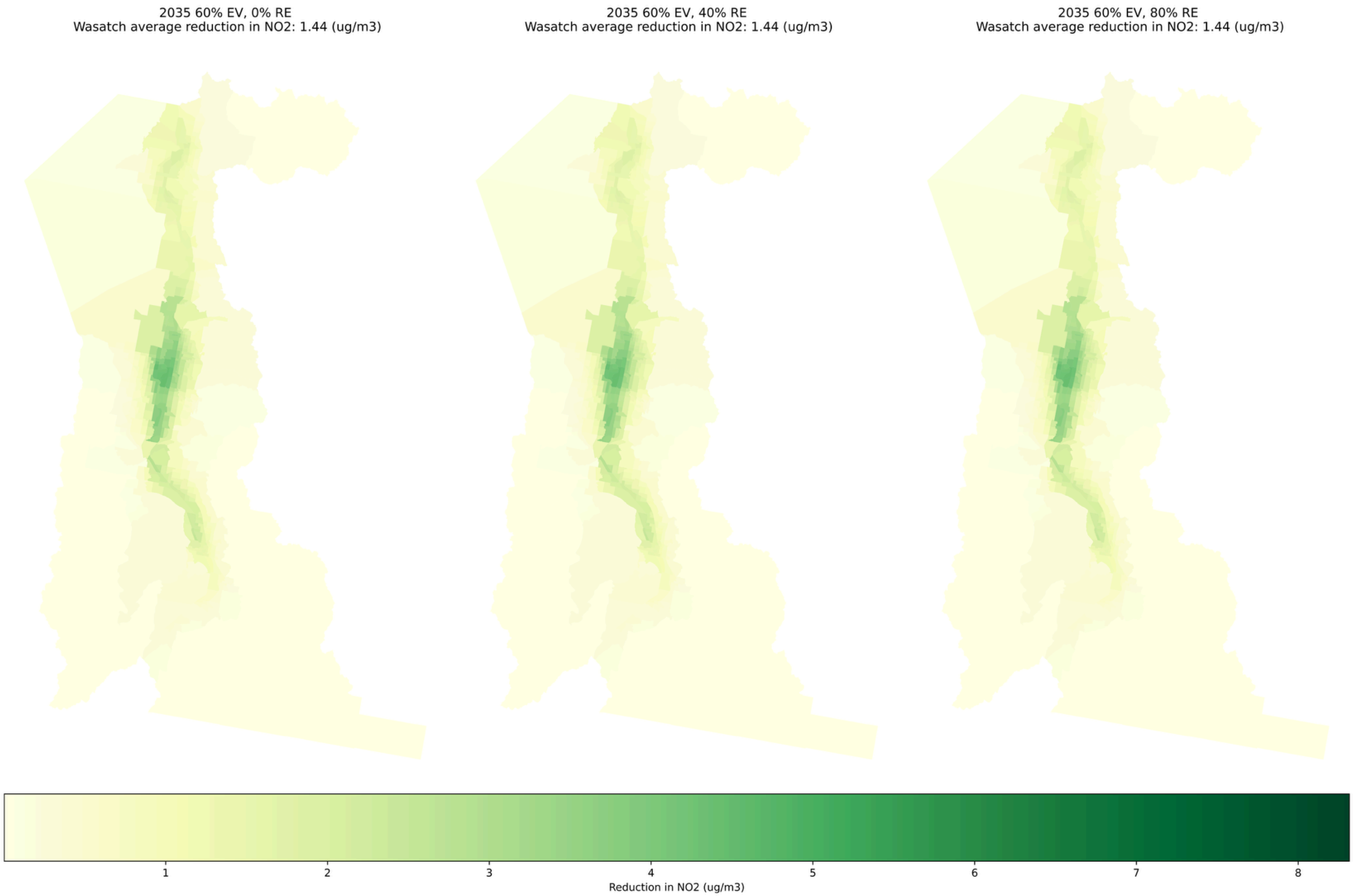

Figure 24: Reductions in NO_2 ($\mu g/m^{-3}$) across the Wasatch Front associated with 60% vehicle electrification powered by 0%, 40%, and 80% renewable energy (RE), 2035

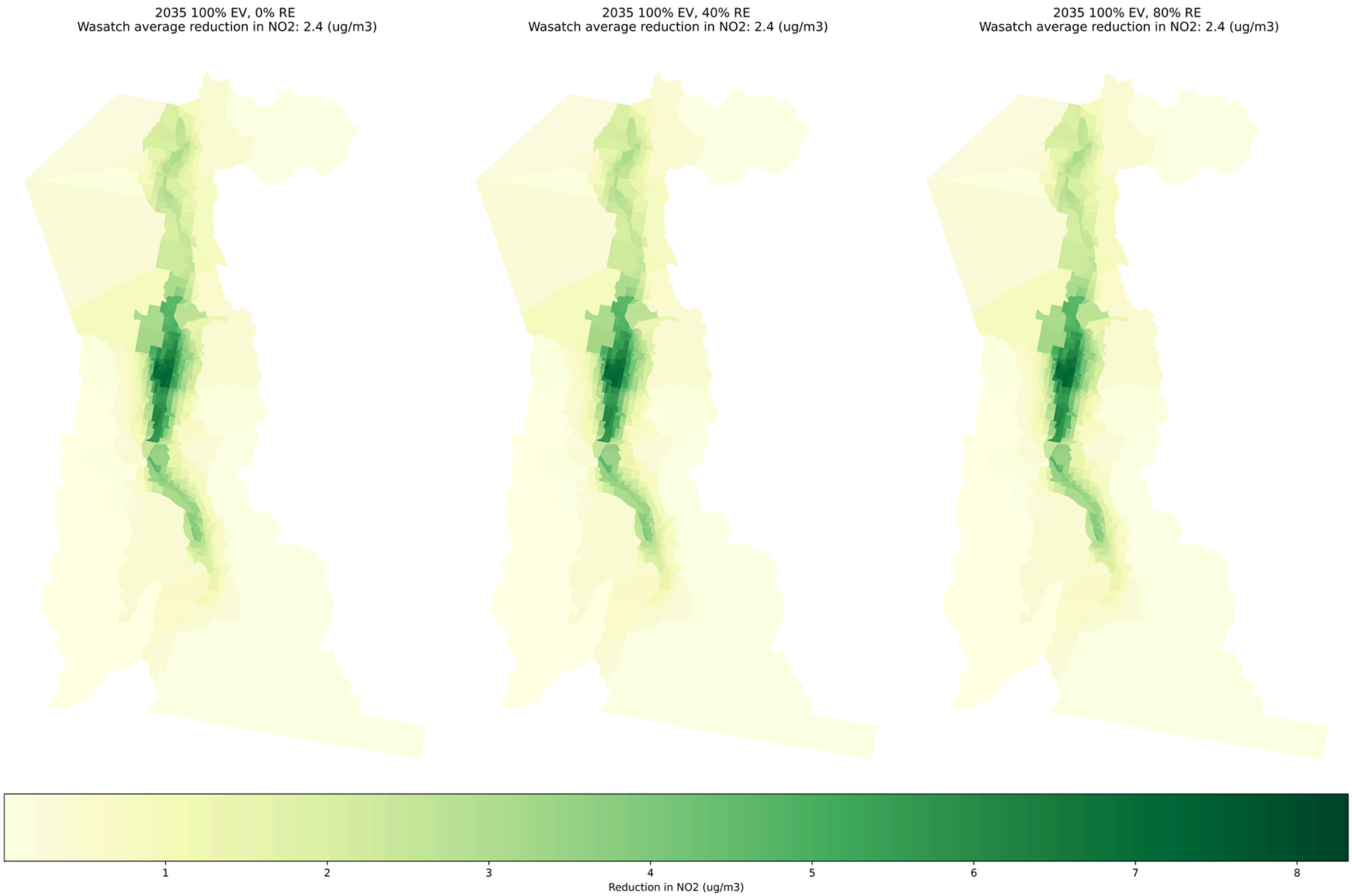

Figure 25: Reductions in NO_2 ($\mu g/m^{-3}$) across the Wasatch Front associated with 100% vehicle electrification powered by 0%, 40%, and 80% renewable energy (RE), 2035

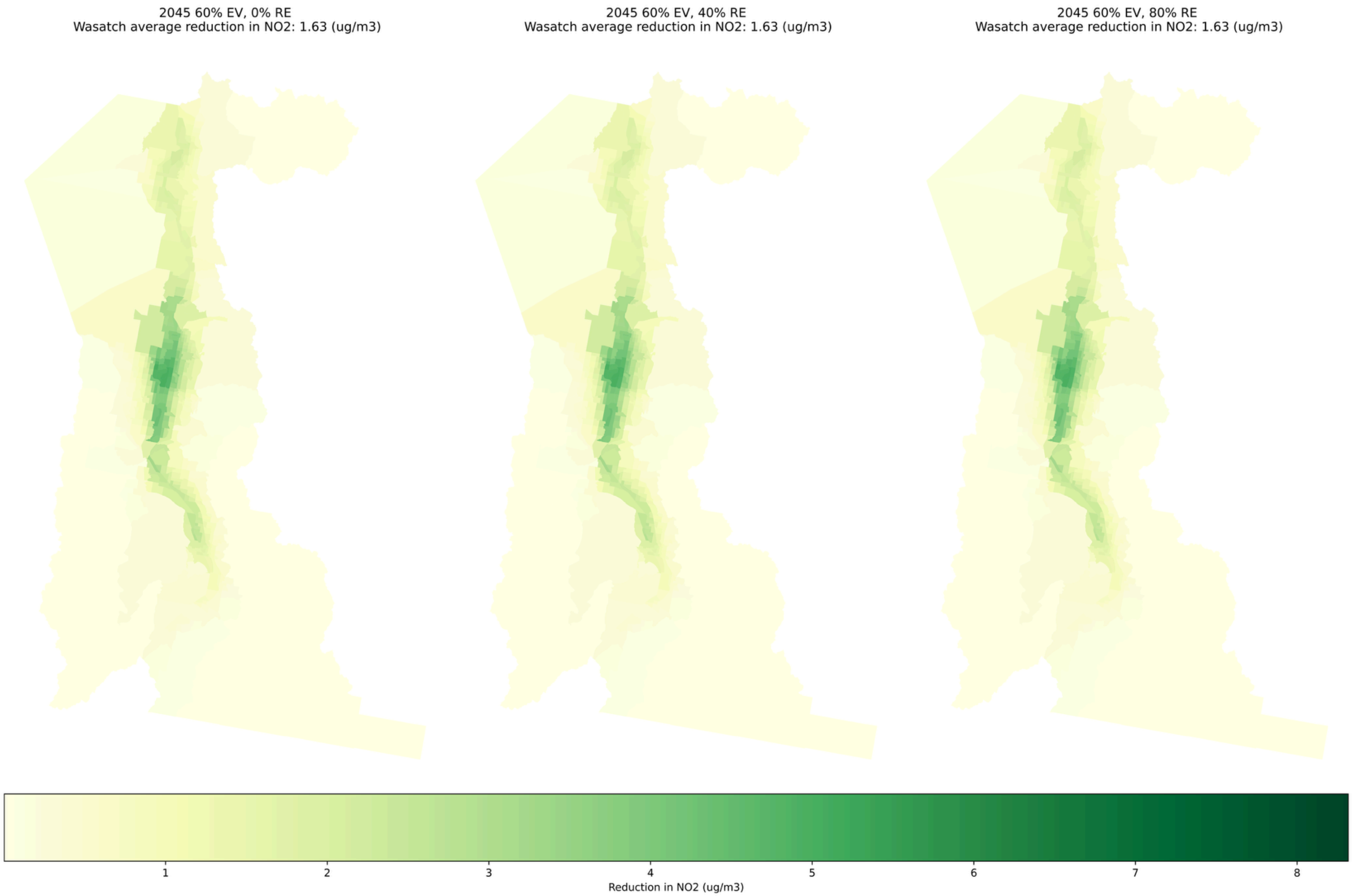

Figure 26: Reductions in NO_2 ($\mu g/m^{-3}$) across the Wasatch Front associated with 60% vehicle electrification powered by 0%, 40%, and 80% renewable energy (RE), 2045

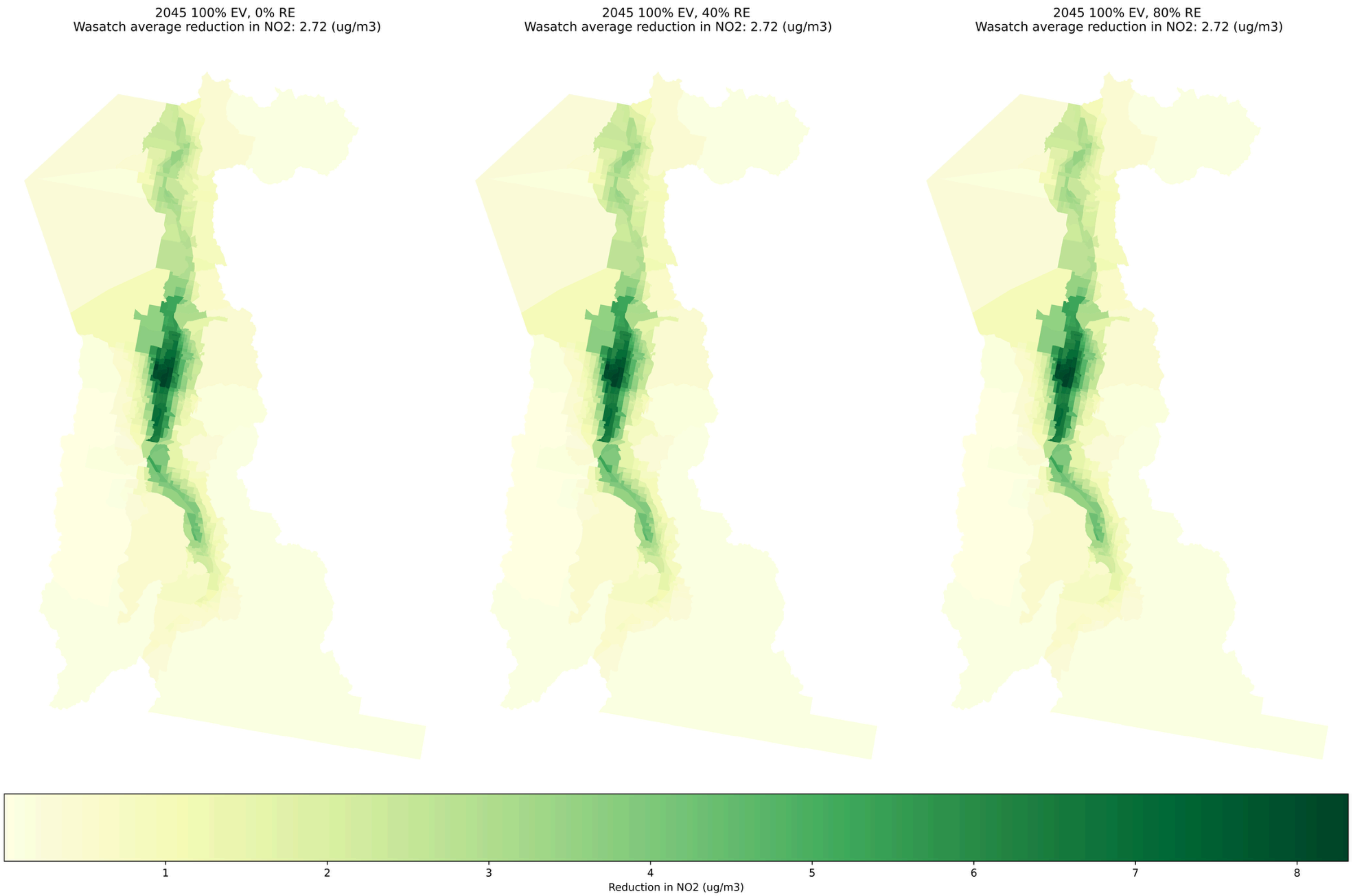

Figure 27: Reductions in NO_2 ($\mu g/m^{-3}$) across the Wasatch Front associated with 100% vehicle electrification powered by 0%, 40%, and 80% renewable energy (RE), 2045

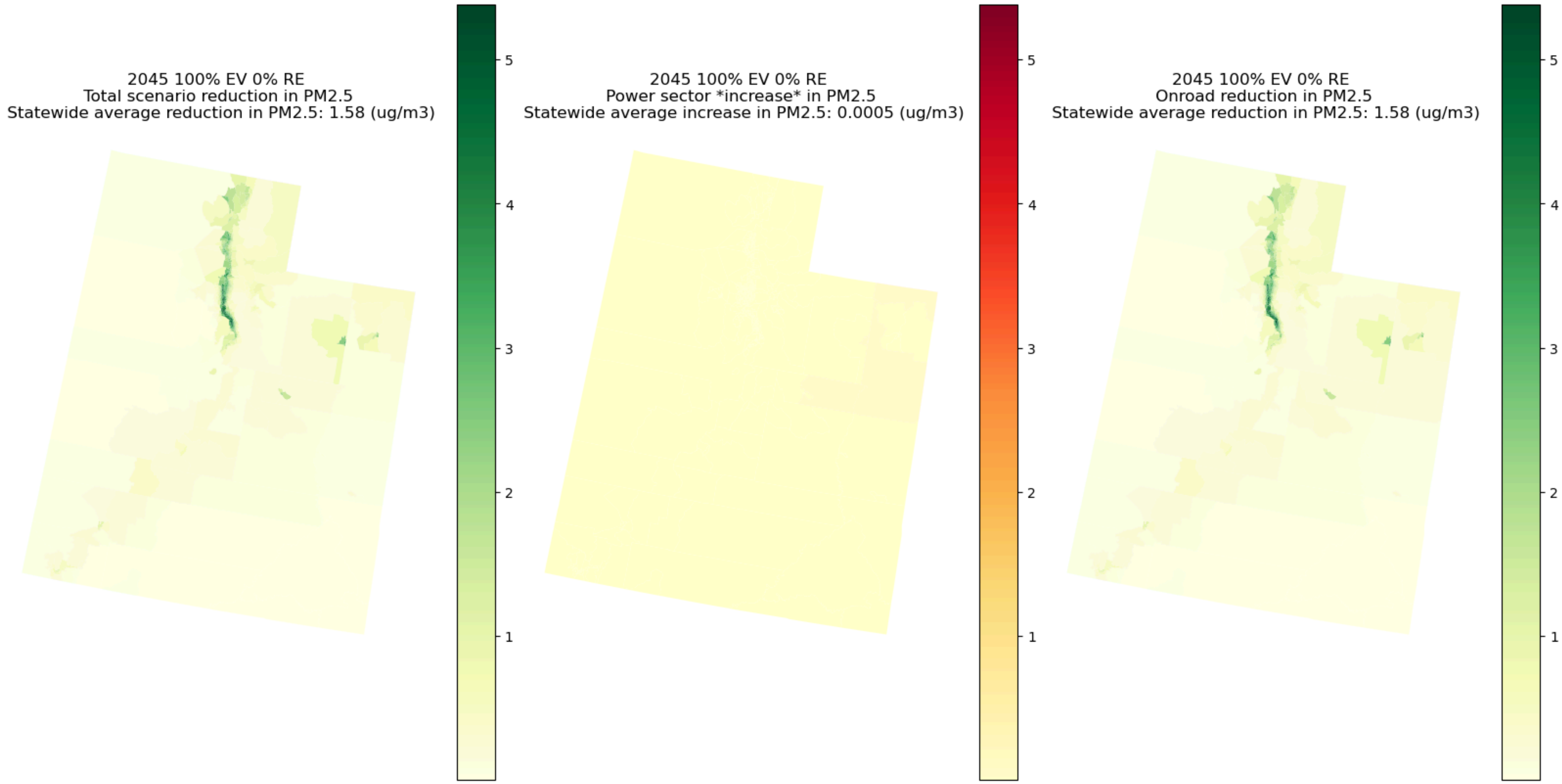

Figure 28: Changes in $PM_{2.5}$ ($\mu g/m^{-3}$) associated with 100% vehicle electrification powered by 0% renewable energy (RE), 2045

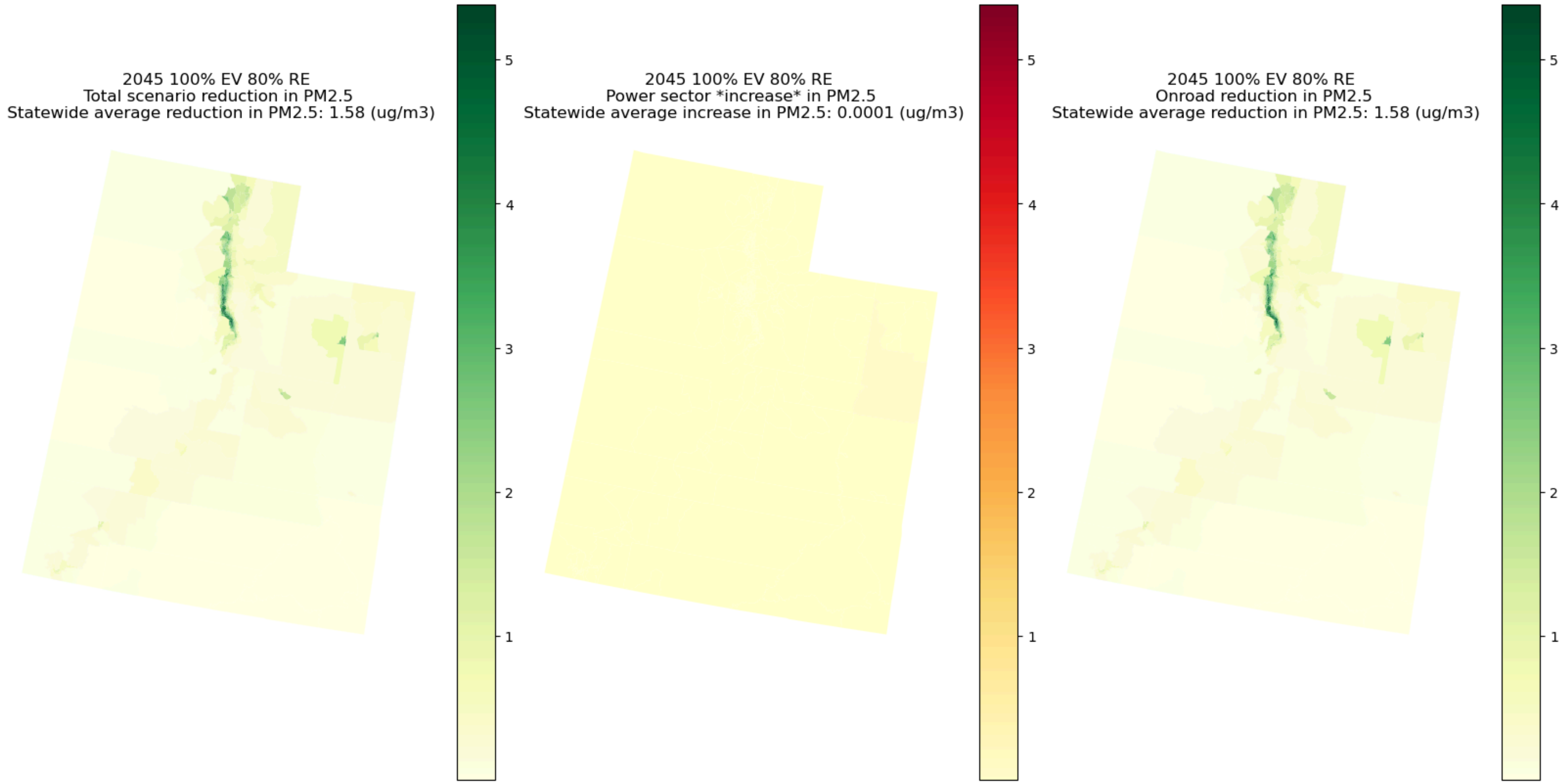

Figure 29: Changes in $PM_{2.5}$ ($\mu g/m^{-3}$) associated with 100% vehicle electrification powered by 80% renewable energy (RE), 2045

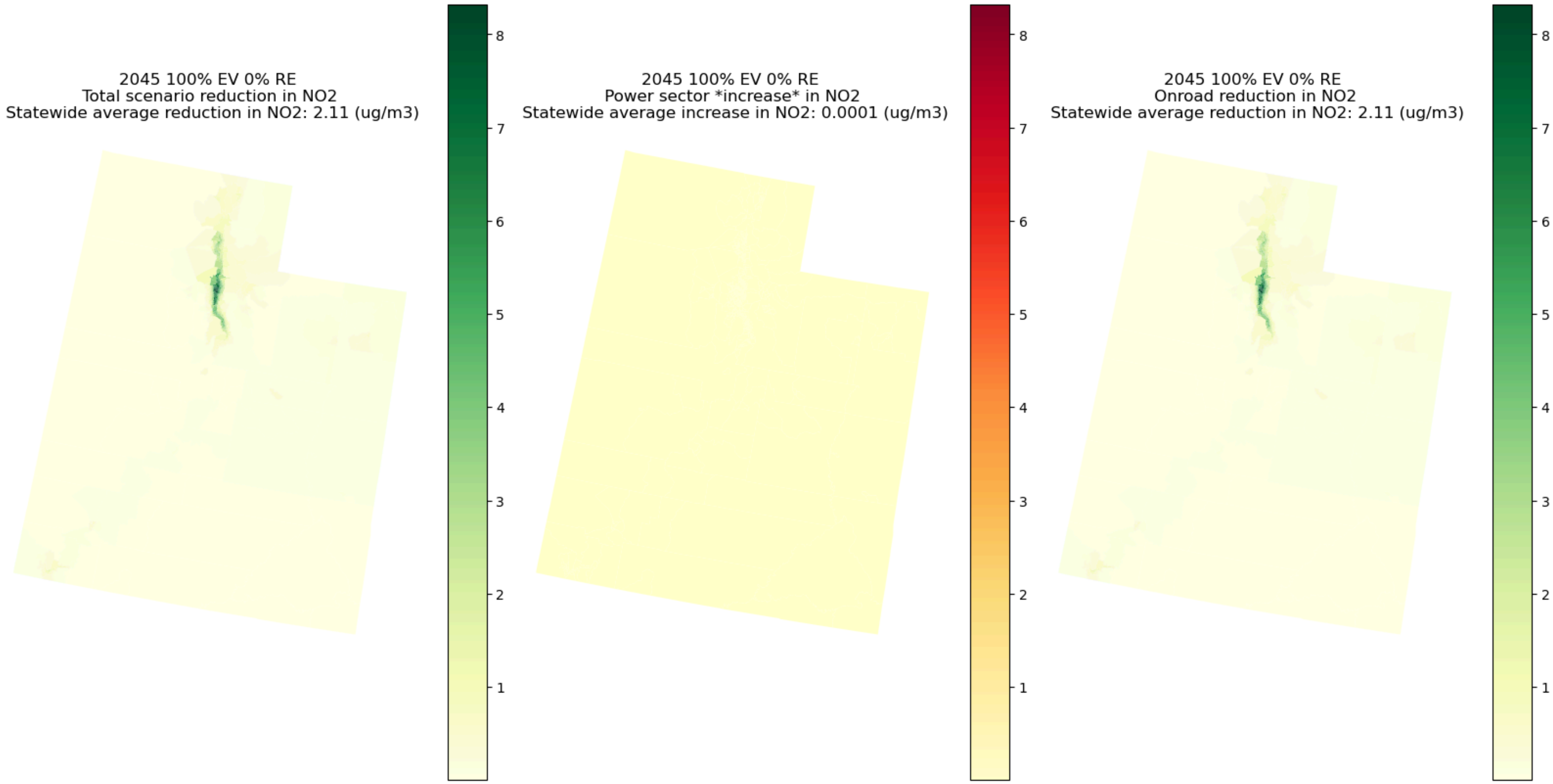

Figure 30: Changes in NO_2 ($\mu g/m^{-3}$) associated with 100% vehicle electrification powered by 0% renewable energy (RE), 2045

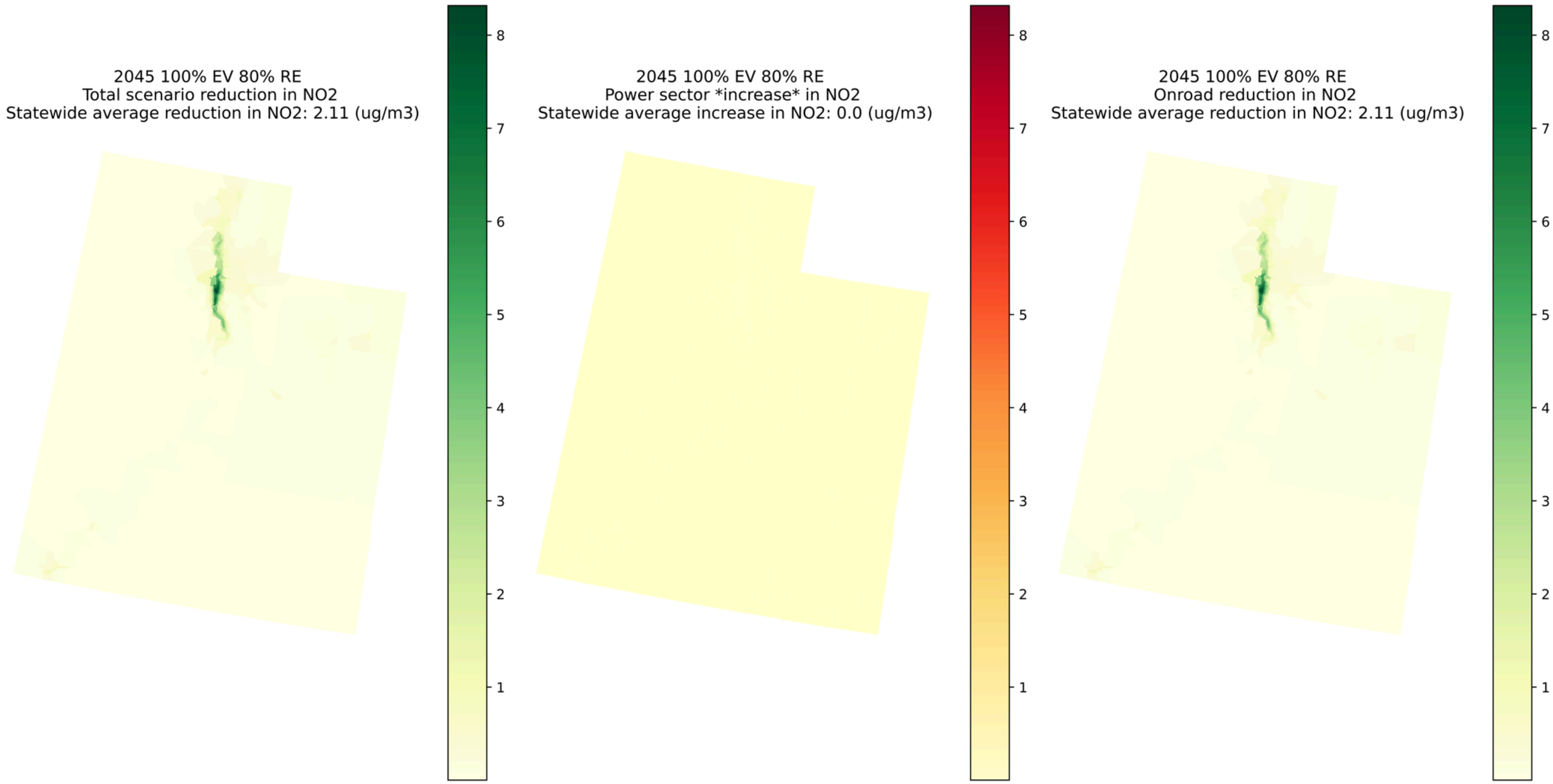

Figure 31: Changes in NO_2 ($\mu g/m^{-3}$) associated with 100% vehicle electrification powered by 80% renewable energy (RE), 2045

Each vehicle electrification scenario resulted in avoided deaths and disease onset (Table 3). In 2025, 100% vehicle electrification could have avoided 103 (95% CI: 60, 137) deaths from $PM_{2.5}$ and 71 (95% CI: 41, 101) from NO_2 annually; by 2045, it could result in 174 (95% CI: 102, 231) avoided deaths from $PM_{2.5}$ and 118 (95% CI: 69, 168) avoided deaths from NO_2 annually. These represent annual avoided mortality, meaning that over a decade, vehicle electrification could lead to over 700 and 1,000 avoided deaths from reduced NO_2 and $PM_{2.5}$ exposure, respectively, based on 2025 assumptions, or over 1,100 and 1,700 deaths from reduced NO_2 and $PM_{2.5}$ exposure, respectively, based on 2045 assumptions. These scenarios were also associated with hundreds of avoided onsets of respiratory diseases (e.g., COPD, asthma), as well as cases of dementia, autism, and diabetes. Avoided morbidity stemming from vehicle electrification can not only reduce healthcare system costs, but it can also lead to quality-of-life improvements for Utahns who never develop chronic conditions that they might have otherwise. These health outcomes—including avoided morbidity—cannot be aggregated because that could lead to double counting: some avoided deaths from $PM_{2.5}$ might also be avoided instances of COPD onset, for example, and the CRFs for each pollutant are not adjusted for one another.

For all scenarios, a majority of the modeled health benefits associated with vehicle electrification were clustered in the Wasatch Front, which features the highest onroad emissions in the state—and therefore, the highest reductions in pollution concentrations for $PM_{2.5}$ and NO_2 associated with vehicle electrification—and a majority of the state's population (Figures 32 - 37).

We did not observe any differences in the modeled health impacts associated with vehicle electrification scenarios based on differences in the power sector (0% RE, 40% RE, 80% RE) (Table 3), although this could have been influenced in part by our assumptions in our power sector modeling (described above and in the discussion section). This indicates that vehicle electrification might lead to avoided deaths and disease onset in Utah provided that vehicle adoption and electricity generation looks very similar to the scenarios explored here. Even when the power sector did produce increases in $PM_{2.5}$ and NO_2 concentrations, these were mitigated by parallel decreases in $PM_{2.5}$ and NO_2 concentrations, even in counties near power plants. As a result, we did not observe any adverse health impacts associated with any vehicle electrification scenario. As with air pollution, the magnitude of modeled health impacts was greater for 100% compared to 60% electrification scenarios and increased in scenarios for future decades.

These results suggest that onroad vehicle emissions contribute significantly to air pollution and the public health burden in the state of Utah, and that policy solutions such as vehicle electrification may help ameliorate some of the state of Utah's air pollution challenges if its implementation resembles the scenarios modeled here.

Table 3: Statewide annual average pollution reductions by pollutant and sector and aggregate avoided deaths and disease onset across scenarios and years

	2025						2035						2045					
	EV100RE0	EV100RE40	EV100RE80	EV60RE0	EV60RE40	EV60RE80	EV100RE0	EV100RE40	EV100RE80	EV60RE0	EV60RE40	EV60RE80	EV100RE0	EV100RE40	EV100RE80	EV60RE0	EV60RE40	EV60RE80
Changes in statewide average PM2.5 and NO2 for each scenario (ug/m3)																		
Avg. total decrease in PM2.5	1.20	1.20	1.20	0.72	0.72	0.72	1.39	1.39	1.39	0.83	0.83	0.83	1.58	1.58	1.58	0.95	0.95	0.95
Avg. total decrease in NO2	1.61	1.61	1.61	0.96	0.96	0.96	1.86	1.86	1.86	1.12	1.12	1.12	2.11	2.11	2.11	1.27	1.27	1.27
Avg. increase in power-sector PM2.5	-0.0004	-0.0002	-0.0001	-0.0002	-0.0001	0.0000	-0.0005	-0.0003	-0.0001	-0.0003	-0.0002	0.0000	-0.0005	-0.0003	-0.0001	-0.0003	-0.0002	-0.0001
Avg. decrease in onroad-sector PM2.5	1.20	1.20	1.20	0.72	0.72	0.72	1.39	1.39	1.39	0.83	0.83	0.83	1.58	1.58	1.58	0.95	0.95	0.95
Avg. increase in power-sector NO2	-0.0001	0.0000	0.0000	0.0000	0.0000	0.0000	-0.0001	0.0000	0.0000	0.0000	0.0000	0.0000	-0.0001	0.0000	0.0000	0.0000	0.0000	0.0000
Avg. decrease in onroad-sector PM2.5	1.61	1.61	1.61	0.96	0.96	0.96	1.86	1.86	1.86	1.12	1.12	1.12	2.11	2.11	2.11	1.27	1.27	1.27
Estimated avoided morbidity and mortality associated with each scenario																		
Dementia	84	84	84	51	51	51	112	112	112	68	68	68	143	143	143	86	86	86
Dementia (low est.)	34	34	34	20	20	20	45	45	45	27	27	27	58	58	58	35	35	35
Dementia (high est.)	147	147	147	89	89	89	195	195	195	118	118	118	249	249	249	151	151	151
Child asthma - PM2.5	69	69	69	41	41	41	92	92	92	56	56	56	118	118	118	71	71	71
Child asthma - PM2.5 (low est	11	11	11	7	7	7	15	15	15	9	9	9	19	19	19	11	11	11
Child asthma - PM2.5 (high es	189	189	189	114	114	114	253	253	253	153	153	153	324	324	324	196	196	196
COPD	183	183	183	110	110	110	243	243	243	146	146	146	311	311	311	187	187	187
COPD (low est.)	107	107	107	65	65	65	143	143	143	86	86	86	183	183	183	110	110	110
COPD (high est.)	273	273	273	164	164	164	363	363	363	219	219	219	464	464	464	280	280	280
Lung cancer	15	15	15	9	9	9	20	20	20	12	12	12	26	26	26	16	16	16
Lung cancer (low est.)	9	9	9	5	5	5	11	11	11	7	7	7	15	15	15	9	9	9
Lung cancer (high est.)	24	24	24	15	15	15	32	32	32	19	19	19	41	41	41	25	25	25
IHD event	25	25	25	15	15	15	33	33	33	20	20	20	42	42	42	25	25	25
IHD event (low est.)	8	8	8	5	5	5	10	10	10	6	6	6	13	13	13	8	8	8
IHD event (high est.)	52	52	52	31	31	31	69	69	69	42	42	42	89	89	89	53	53	53
Stroke	12	12	12	7	7	7	16	16	16	10	10	10	21	21	21	12	12	12
Stroke (low est.)	8	8	8	5	5	5	10	10	10	6	6	6	13	13	13	8	8	8
Stroke (high est.)	18	18	18	11	11	11	24	24	24	14	14	14	30	30	30	18	18	18
Diabetes	53	53	53	32	32	32	70	70	70	42	42	42	90	90	90	54	54	54
Diabetes (low est.)	13	13	13	8	8	8	17	17	17	10	10	10	22	22	22	13	13	13
Diabetes (high est.)	113	113	113	68	68	68	151	151	151	91	91	91	192	192	192	116	116	116
Autism	61	61	61	37	37	37	82	82	82	50	50	50	105	105	105	64	64	64
Autism (low est.)	7	7	7	4	4	4	10	10	10	6	6	6	13	13	13	8	8	8
Autism (high est.)	249	249	249	151	151	151	332	332	332	202	202	202	425	425	425	259	259	259
Child asthma - NO2	28	28	28	17	17	17	37	37	37	22	22	22	47	47	47	29	29	29
Child asthma - NO2 (low est.)	7	7	7	4	4	4	9	9	9	6	6	6	12	12	12	7	7	7
Child asthma - NO2 (high est.	80	80	80	48	48	48	107	107	107	64	64	64	136	136	136	82	82	82
Adult asthma -NO2	65	65	65	39	39	39	85	85	85	51	51	51	108	108	108	65	65	65
Adult asthma - NO2 (low est.)	5	5	5	3	3	3	7	7	7	4	4	4	9	9	9	5	5	5
Adult asthma - NO2 (high est.	162	162	162	98	98	98	214	214	214	129	129	129	271	271	271	164	164	164
ALRI	20	20	20	12	12	12	27	27	27	16	16	16	34	34	34	20	20	20
ALRI (low est.)	8	8	8	5	5	5	11	11	11	7	7	7	14	14	14	9	9	9
ALRI (high est.)	28	28	28	17	17	17	37	37	37	22	22	22	47	47	47	28	28	28
Mortality - PM2.5	103	103	103	62	62	62	136	136	136	82	82	82	174	174	174	105	105	105
Mortality - PM2.5 (low est.)	60	60	60	36	36	36	80	80	80	48	48	48	102	102	102	62	62	62
Mortality - PM2.5 (high est.)	137	137	137	82	82	82	181	181	181	109	109	109	231	232	232	139	139	139
Mortality - NO2	71	71	71	42	42	42	93	93	93	56	56	56	118	118	118	71	71	71
Mortality - NO2 (low est.)	41	41	41	25	25	25	55	55	55	33	33	33	69	69	69	42	42	42
Mortality -NO2 (high est.)	101	101	101	61	61	61	133	133	133	80	80	80	168	168	168	101	101	101

Figure 32: Statewide avoided deaths and disease onset associated with 60% (L) and 100% (R) reductions in $PM_{2.5}$ emmissions in vehicle electrification scenario, 2025. We do not present other power sector scenarios (0%, 40%, 80% renewable energy (RE)) because there was no difference in avoided health impacts across these scenarios

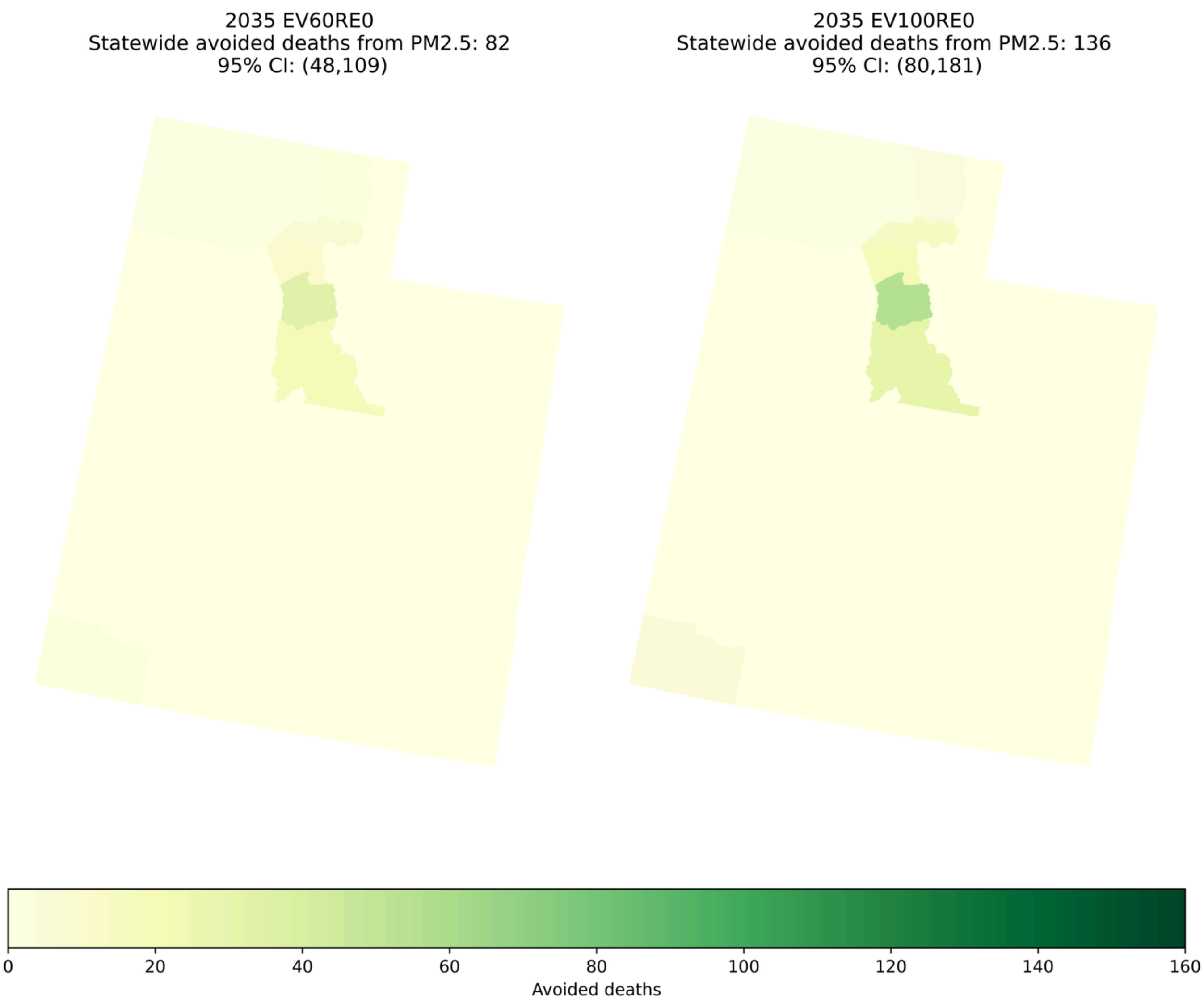

Figure 33: Statewide avoided deaths and disease onset associated with 60% (L) and 100% (R) reductions in $PM_{2.5}$ emmissions in vehicle electrification scenario, 2035. We do not present other power sector scenarios (0%, 40%, 80% renewable energy (RE)) because there was no difference in avoided health impacts across these scenarios

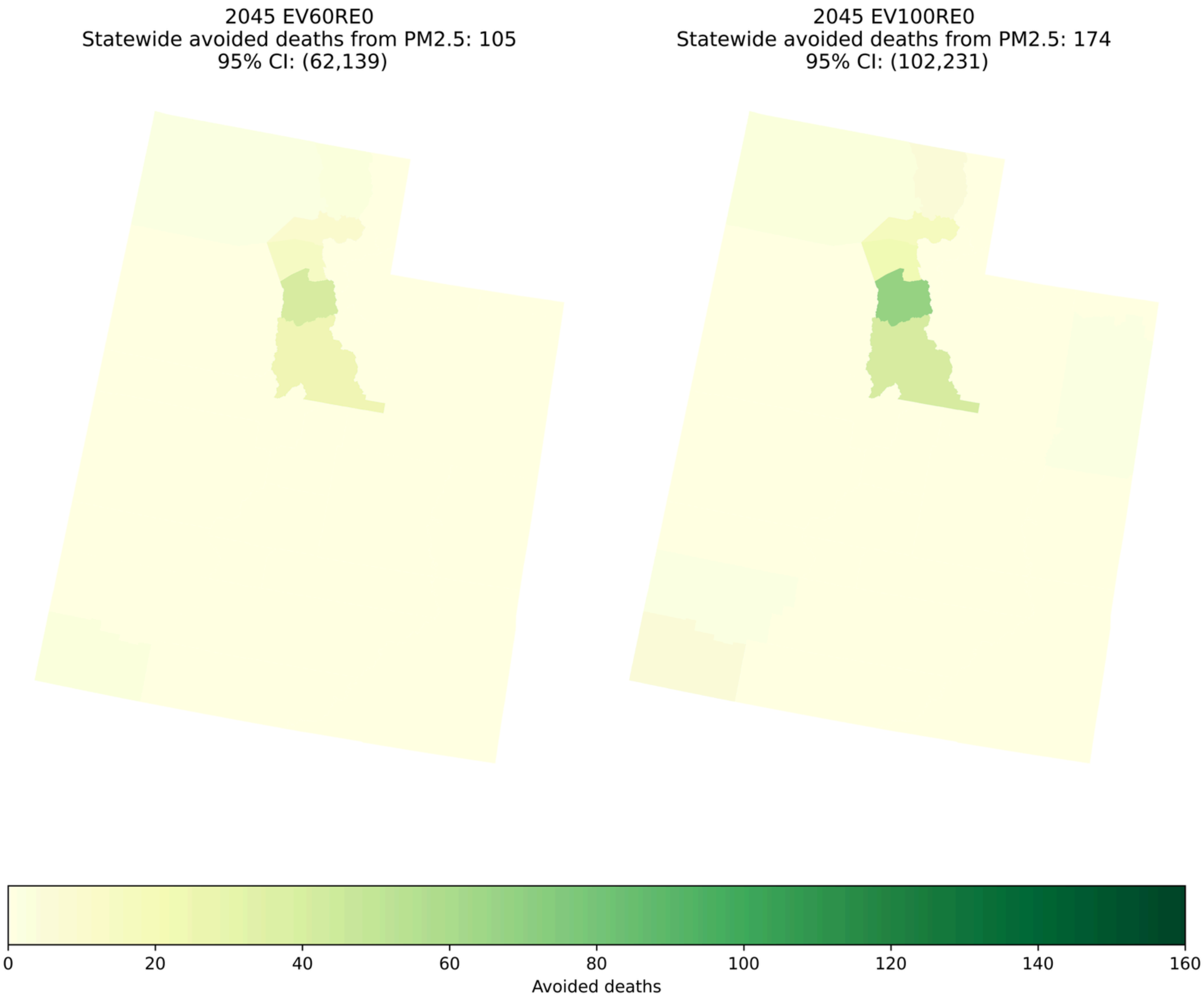

Figure 34: Statewide avoided deaths and disease onset associated with 60% (L) and 100% (R) reductions in $PM_{2.5}$ emmissions in vehicle electrification scenario, 2045. We do not present other power sector scenarios (0%, 40%, 80% renewable energy (RE)) because there was no difference in avoided health impacts across these scenarios

Figure 35: Statewide avoided deaths and disease onset associated with 60% (L) and 100% (R) reductions in NO_2 emmissions in vehicle electrification scenario, 2025. We do not present other power sector scenarios (0%, 40%, 80% renewable energy (RE)) because there was no difference in avoided health impacts across these scenarios.

Figure 36: Statewide avoided deaths and disease onset associated with 60% (L) and 100% (R) reductions in NO_2 emmissions in vehicle electrification scenario, 2035. We do not present other power sector scenarios (0%, 40%, 80% renewable energy (RE)) because there was no difference in avoided health impacts across these scenarios.

Figure 37: Statewide avoided deaths and disease onset associated with 60% (L) and 100% (R) reductions in NO_2 emmissions in vehicle electrification scenario, 2045. We do not present other power sector scenarios (0%, 40%, 80% renewable energy (RE)) because there was no difference in avoided health impacts across these scenarios.

3 Discussion

Our findings suggest that vehicle electrification in Utah could lead to reduced $PM_{2.5}$ and NO_2 concentrations and hundreds of instances of avoided morbidity and mortality annually, amounting to thousands of avoided deaths and cases of disease onset over a decade provided that *electric vehicle adoption and electricity generation look very similar to the scenarios modeled here*. These benefits are expected to increase over time due to projected increases in Utah's population, driving tandem increases in vehicle traffic and onroad emissions that could be offset by electrifying those vehicles; roughly 35-40% vehicle electrification by 2045 would keep onroad emissions equivalent with 2019 onroad emissions. Spatially, $PM_{2.5}$ and NO_2 pollution reductions and associated avoided morbidity and mortality were clustered along the Wasatch Front and relatively sparse across the rest of the state; this is likely due to the spatial patterning of densely trafficked highways—where the air pollution impacts of reduced onroad emissions would accumulate—surrounded by population clusters. We found that higher levels of vehicle electrification (100% versus 60%) were associated with more avoided instances of death and disease onset, regardless of the power sector scenario, because the magnitude of onroad $PM_{2.5}$ and NO_2 reductions outweighed increases in $PM_{2.5}$ and NO_2 pollution associated with the power sector. It is worth noting that a relatively small proportion of added load was met by in-state coal-fired power plants, and that increased reliance on in-state power generation from coal-fired power plants could change the relative balance of health benefits and health harms. We observed a negligible difference in $PM_{2.5}$ and NO_2 concentrations across different power sector scenarios (e.g. 0% of added load powered by renewable energy versus 80% of added load powered by renewable energy), resulting in no discernable differences in avoided health outcomes between these scenarios. These results suggest that vehicle electrification in Utah could lead to substantial air quality and public health improvements at high adoption levels.

3.1 Comparison to Past Studies and Contribution to Literature

Our study contributes to a growing body of evidence exploring the health impacts of vehicle electrification. A recent review of the health impacts of vehicle electrification found that most studies have found vehicle electrification to positively impact public health, which agrees with our study's conclusion (Pennington et al., 2024). Despite different underlying assumptions, our results are comparable to the avoided mortality estimates simulated by Pan et al. (2023) for almost complete electrification of passenger electric vehicles in Salt Lake City in 2050; they estimate 33 avoided deaths associated with reductions in passenger vehicle PM2.5, we estimate 68 across light- and heavy-duty vehicles across the county. Other investigations that use fine spatial resolution air pollution data to conduct HIAs of the impacts of vehicle electrification in Chicago, IL found that the avoided health impacts associated with NO_2 outnumbered those associated with $PM_{2.5}$ (Camilleri et al., 2023; Visa et al., 2023), which we did not find. This could be attributable to different ways of estimating NO_2 concentrations —they used a CTM—different modeling domains with a different spatial patterning of vehicle emissions and population clusters, and assumptions underlying our onroad emissions inventories; it's worth noting that they utilize 2016 NEI data projected from the 2014 NEI, whereas we use future-projected agent-based onroad emissions inventories. The Camilleri et al. (2023) and Visa et al. (2023) studies also found a larger magnitude of avoided mortality for scenarios featuring a lower penetration of electric vehicles, although they did use Census tract-level mortality rates, and found that some areas with the largest numbers of avoided death were not those with the largest reductions in air pollution concentrations, which could explain some of the difference in our results. However, Choma et al. (2020) did find that the avoided mortality impacts in Chicago were much higher than in Salt Lake City due to the magnitude of emissions change and the spatial patterning of population relative to emissions, which could also explain some of this difference.

Some vehicle electrification studies found that improving air pollution concentrations in dense, urban areas came at the cost of worsening air pollution around power plants (Pennington et al., 2024), but we did not observe this phenomenon in our study. This could be because a large proportion of the added power load associated with EV adoption (31-41%, depending on the scenario) was assumed to be met by power plants outside of Utah (although they were included in the modeling), and therefore had a limited impact on air pollution concentrations in the state. It could also be because a large proportion of added power load assigned to fossil fuel plants within Utah was assumed to be met by natural gas rather than coal-fired plants (54-70%, depending on the scenario), and natural gas plants have a smaller impact on human health outcomes than coal-fired electricity generation power plants (Buonocore et al., 2021; Lueken et al., 2016). Similar to our findings, Camilleri et al. (2023) and Visa et al. (2023) found that reductions in $PM_{2.5}$ and NO_2 associated with the onroad sector outweighed power sector increases even in Census tracts with power plants, which supports our finding, although they considered lower penetration of electric vehicles (heavy-duty only and 30% electrification, respectively) and therefore, a lower increase in additional power generation. *Our study's finding that vehicle electrification produced minimal increases in power-sector $PM_{2.5}$ and NO_2 concentrations should not be seen as indicating that vehicle electrification never produces increased air pollution associated with the power sector, which has been documented in past studies (Schnell et al., 2019; Weis et al., 2016), just that it did not in these scenarios.* The health impacts of vehicle electrification are highly tied to the spatial patterning of population centers, roadways, and power generation resources, as well as the underlying assumptions about where vehicles will be electrified and what sources will power them, and results may look much different in places with different spatial patterning of these features or under different adoption or power generation scenarios.

Our study offers several contributions to the literature. It is the first study, to our knowledge, to estimate NO_2 concentrations from InMAP outputs using NO_2:NO_x ratios. Typically, reduced complexity modeling is used to estimate $PM_{2.5}$ concentrations alone, which limits the scope of air pollution that can be considered with these tools. By including NO_2, we hope to expand the scope of what's possible with RCMs, making consideration of additional pollutants applicable to practitioners that lack the experience or computing power to run a full CTM, or who are interested in the spatial resolution advantages of a tool like InMAP.

Our study is not the only one to model the impacts of vehicle electrification with a roughly ~1km output grid cell (Camilleri et al., 2023; Visa et al., 2023), but to our knowledge, it is the first vehicle electrification study conducted with InMAP to utilize a 1x1 km input emissions and output air pollution concentrations at a uniform 1x1 km spatial resolution. The combination of high spatial resolution input data and output resolution have been found to produce the most accurate InMAP outputs in previous evaluations (Rieves et al., *in preparation*), and to produce the most accurate air pollution and health impacts in other studies (Paolella et al., 2018; Vodonos & Schwartz, 2021). Our study also includes a more diverse set of health endpoints than most other studies which focus predominantly on impacts to mortality or one or two health endpoints (Pennington et al., 2024), whereas we included 11 morbidity endpoints. Our study is also unique in the vehicle electrification literature for quantifying uncertainty for more than the CRF (Pennington et al., 2024). On the emissions modeling side, we utilized detailed agent-based modeling to create future-projected onroad emissions inventories based on more realistic assumptions about where within Utah electric vehicles (EVs) would be adopted rather than spatially downscaling a past inventory using spatial surrogates (Camilleri et al., 2023; Visa et al., 2023) or assuming spatially uniform EV adoption at the county level, which is common in past studies (Choma et al., 2020; Pan et al., 2023). We also considered multiple power sector scenarios per year, allowing us to understand the impact of electric generation sources and scenarios on air pollution and health outcomes. Using future-projected inventories of the power sector does introduce uncertainty—especially for the power sector, where questions about load growth from other sources, like data centers and AI, could substantially change the power sector landscape—but does retain more policy salience than using a past year as a baseline.

3.2 Limitations

Despite several notable advantages to our modeling approach, our work is not without limitations. Any HIA is subject to substantial uncertainty at each stage of the modeling process. We tried our best to account for this whenever possible by including 95% confidence intervals to create "uncertainty estimates" based on the upper and lower estimates for each CRF and incidence rates but could not do so for projected population data and modeled air pollution concentrations. Because of the considerable uncertainty they entail, HIA results should be considered estimates of the *magnitude and direction* of potential health impacts rather than a specific outcome, and results should be interpreted accordingly. HIA results such as avoided deaths and onset of disease cannot be added together, as some avoided deaths from $PM_{2.5}$ might also be avoided deaths from NO_2 or avoided instances of lung cancer onset, for example; this means that results cannot communicate an aggregate health burden across conditions, although they can communicate the myriad health impacts of air pollution exposure that might be avoided through vehicle electrification.

Furthermore, there are limitations with the administrative data used in this work. Some of the age ranges for incidence or population data do not precisely line up with the age range listed for some CRFs, although we use the closest interval whenever this arose (Appendix 1). Incidence data was not yet available for our baseline year (2025), so we used data from most recent year data that we could find for GBD (2023) and CDC WONDER (2024) data instead. Some data was also not available at the spatial resolution we wanted: incidence rates were only available for morbidity at the statewide extent (for mortality, they were available at the county). This obscures the fact that the incidence rate varies across a population which impacts the likelihood of death or disease onset from air pollution exposure, but we were unable to capture this nuance in this case. Past studies have found that variations in underlying mortality rates at a finer spatial scale influenced results, with some tracts with lower reductions in air pollution still experienced higher numbers of avoided deaths due to the higher underlying mortality rates (Visa et al., 2023; Vodonos & Schwartz, 2021). Using finer resolution incidence data could change our results but was not something we explored in this study.

Another limitation in our analysis is that our modeled air pollution concentrations are likely lower —especially for the power sector—than they would be in reality. InMAP has biases, notably it underpredicts pSO_4 *(Gallagher et al., 2023; Paolella et al., 2018; Rieves et al., in preparation*; Tessum et al., 2017). Because pSO_4 is tied to energy generation, this suggests that our modeled air pollution concentrations and health impacts from the power sector may be an underrepresentation of the true burden associated with it. We tried to mitigate this bias by correcting the particulate components of $PM_{2.5}$ using previously published correction factors for the state of Utah (Gallagher et al., 2023). Additionally, InMAP struggles to estimate the long-range fate and transport of pollution across smaller grid cells for several reasons. InMAP's algorithm for modeling long-range fate and transport is implicitly tied to grid cell size, as InMAP assumes higher wind speeds in larger grid cells (Tessum et al., 2017); assuming a lower windspeed likely underpredicts the transport of air pollution. InMAP also calculates transport based on neighbors rather than distance (Tessum et al., 2017), meaning that large cells surrounded by large cells reflect diffusion across a larger geographical extent than small cells surrounded by small cells. This can lead to underprediction in areas characterized by non-ground level—such as power plant—emissions sources (Rieves et al., *in preparation*). In instances where InMAP did predict noticeable impacts in air pollution associated with electric generation, aggregating predicted $PM_{2.5}$ concentrations from a 1x1 km grid cell to the Census tract "averaged out" some of the extreme values near power plants, reducing the maximum power plant-related $PM_{2.5}$ concentrations from 0.2 to 0.08 $\mu g/m^{-3}$, which is an unfortunate impact of rural areas having larger Census tract sizes and reflects the fact that spatial data is sensitive to the boundaries in which it is aggregated (Jerrett et al., 2010). It is possible that some near power-plant communities could experience larger increases than decreases in $PM_{2.5}$ pollution, resulting in adverse health impacts, but this was not evident at the spatial unit of our analysis. All of this suggests that our estimation of the air pollution concentrations and associated health impacts from power plants may be under-estimated in this work, although we have done our best through correction to ameliorate these concerns.

Our NO_2 concentrations are also uncertain, as they are not directly modeled, but are estimated by applying an NO_2:NO_x ratio to modeled NO_x concentrations. This means that NO_2 concentrations presented here should be thought of as a rough estimate, which is suitable for this type of modeling in general, meant to convey the expected magnitude and direction of impacts rather than specific number. We did not correct NO_2 concentrations because there were not previously published scaling factors for the state of Utah, but future work should explore the impact of correcting InMAP-output NO_2**.**

We estimated the health impacts associated with annual average concentrations of $PM_{2.5}$ and NO_2, and although the annual average implicitly accounts for all air pollution, it smooths out potential impacts of extremes. Some studies have explored the relationship between high episodic $PM_{2.5}$ exposure and health outcomes like mortality (Yu et al., 2024). However, such investigations are not applicable here, as these only apply to previously observed or short term forecasted air pollution concentrations, instead of long-range forward-looking scenarios. This is because we cannot use emissions to simulate future short term air pollution dynamics—like inversions—outside of the immediate future due to the large uncertainty it would invite. Past work has found that during meteorological inversions air pollution from highly local sources are the biggest concern due to low windspeeds (Silberstein et al., 2024), thus it is possible that vehicle electrification could ameliorate some of the severity of $PM_{2.5}$ concentrations during inversion periods for communities near roadways, although this is outside the scope of this study.

Despite these limitations, our study provides a robust accounting of the potential health impacts of $PM_{2.5}$ and NO_2 across the state of Utah. We consider 18 different scenarios of varying degrees of electric vehicle adoption and electric generation conditions from now until 2045, leveraging fine spatial scale emissions to project air pollution concentrations and using detailed underlying health data and rigorous CRFs to estimate avoided all-cause mortality and morbidity across 11 different endpoints across. The goal of this work was to provide the state of Utah with a reasonable estimate of the direction and magnitude of potential air pollution and health impacts of vehicle electrification scenarios. Our results indicate that high levels of vehicle electrification in Utah may lead to substantial reductions in $PM_{2.5}$ and NO_2 pollution, especially within the Wasatch Front, resulting in hundreds of instances of avoided deaths and disease onset across myriad conditions *if electric vehicle adoption and electricity generation look very similar to the scenarios modeled here*. These results are incredibly sensitive to underlying assumptions, however, and our study's finding that vehicle electrification produced minimal increases in power-sector $PM_{2.5}$ and NO_2 concentrations is reflective of the specific power systems scenarios we considered in these analyses and may not hold under markedly different assumptions about the power sector.

4 Conclusion

High levels of EV adoption may help avoid death and disease onset in the state of Utah, particularly in the Wasatch Front if electric vehicle adoption and electricity generation look very similar to the scenarios modeled here. Avoided deaths and disease onset are greatest for 100% compared to 60% vehicle electrification scenarios and are highest in future years due to projected increases in population and traffic volume. As modeled here, the power sector did not contribute to noticeable increases in PM2.5 and NO2 concentrations, although this could be due to the relatively low amount of in-state coal fired generation included in our power systems scenarios. Overall, these results are sensitive to model assumptions —the type and location of additional electric generation, where and how many EVs are adopted —and should not be considered universal.

5 References

Amos, H. M., Skaff, N. K., Schollaert Uz, S., Policelli, F. S., Slayback, D., Macorps, E., Jo, M. J., Patel, K., Keller, C. A., Abue, P., Buchard, V., & Werner, A. K. (2023). Public Health Data Applications Using the CDC Tracking Network: Augmenting Environmental Hazard Information With

Lower-Latency NASA Data. *GeoHealth*, *7*(12), e2023GH000971. https://doi.org/10.1029/2023GH000971

Anenberg, S. C., Belova, A., Brandt, J., Fann, N., Greco, S., Guttikunda, S., Heroux, M.-E., Hurley, F., Krzyzanowski, M., Medina, S., Miller, B., Pandey, K., Roos, J., & Van Dingenen, R. (2016). Survey of Ambient Air Pollution Health Risk Assessment Tools. *Risk Analysis: An Official Publication of the Society for Risk Analysis*, *36*(9), 1718–1736. https://doi.org/10.1111/risa.12540

Baker, K. R., Amend, M., Penn, S., Bankert, J., Simon, H., Chan, E., Fann, N., Zawacki, M., Davidson, K., & Roman, H. (2020). A database for evaluating the InMAP, APEEP, and EASIUR reduced complexity air-quality modeling tools. *Data in Brief*, *28*, 104886. https://doi.org/10.1016/j.dib.2019.104886

Boylan, J. W., & Russell, A. G. (2006). PM and light extinction model performance metrics, goals, and criteria for three-dimensional air quality models. *Atmospheric Environment, Special Issue on Model Evaluation: Evaluation of Urban and Regional Eulerian Air Quality Models*, *40*(26), 4946–4959. https://doi.org/10.1016/j.atmosenv.2005.09.087

Buonocore, J. J., Salimifard, P., Michanowicz, D. R., & Allen, J. G. (2021). A decade of the U.S. energy mix transitioning away from coal: Historical reconstruction of the reductions in the public health burden of energy. *Environmental Research Letters*, *16*(5), 054030. https://doi.org/10.1088/1748-9326/abe74c

Camilleri, S. F., Montgomery, A., Visa, M. A., Schnell, J. L., Adelman, Z. E., Janssen, M., Grubert, E. A., Anenberg, S. C., & Horton, D. E. (2023). Air quality, health and equity implications of electrifying heavy-duty vehicles. *Nature Sustainability*, 1–11. https://doi.org/10.1038/s41893-023-01219-0

Center for Disease Control and Prevention. (n.d.). *CDC WONDER*. Retrieved April 11, 2023, from https://wonder.cdc.gov/controller/datarequest/D76

Choma, E. F., Evans, J. S., Hammitt, J. K., Gómez-Ibáñez, J. A., & Spengler, J. D. (2020). Assessing the health impacts of electric vehicles through air pollution in the United States. *Environment International*, *144*, 106015. https://doi.org/10.1016/j.envint.2020.106015

Crooks, J. L., & Özkaynak, H. (2014). Simultaneous statistical bias correction of multiple PM2.5 species from a regional photochemical grid model. *Atmospheric Environment*, *95*, 126–141. https://doi.org/10.1016/j.atmosenv.2014.06.024

Diao, M., Holloway, T., Choi, S., O'Neill, S. M., Al-Hamdan, M. Z., Van Donkelaar, A., Martin, R. V., Jin, X., Fiore, A. M., Henze, D. K., Lacey, F., Kinney, P. L., Freedman, F., Larkin, N. K., Zou, Y., Kelly, J. T., & Vaidyanathan, A. (2019). Methods, availability, and applications of PM2.5 exposure estimates derived from ground measurements, satellite, and atmospheric models. *Journal of the Air & Waste Management Association*, *69*(12), 1391–1414. https://doi.org/10.1080/10962247.2019.1668498

Forastiere, F., Spadaro, J. V., Ancona, C., Jovanovic Andersen, Z., Cozzi, I., Gumy, S., Loncar, D., Mudu, P., Medina, S., Perez Velasco, R., Walton, H., Zhang, J., & Krzyzanowski, M. (2024). Choices of morbidity outcomes and concentration-response functions for health risk assessment of long-term exposure to air pollution. *Environmental Epidemiology*, *8*(4), e314. https://doi.org/10.1097/EE9.0000000000000314

Gallagher, C. L., Holloway, T., Tessum, C. W., Jackson, C. M., & Heck, C. (2023). Combining Satellite-Derived PM2.5 Data and a Reduced-Form Air Quality Model to Support Air Quality Analysis in US Cities. *GeoHealth*, *7*(5), e2023GH000788. https://doi.org/10.1029/2023GH000788

Institute for Health Metrics and Evaluation. (2025). *GBD Results* [Dataset]. https://www.healthdata.org/data-tools-practices/interactive-visuals/gbd-results

Jackson, C. M., Holloway, T., & Tessum, C. W. (2023). City-scale analysis of annual ambient PM2.5 source contributions with the InMAP reduced-complexity air quality model: A case study of Madison, Wisconsin. *Environmental Research: Infrastructure and Sustainabil-*

ity, *3*(1), 015002. https://doi.org/10.1088/2634-4505/acb0fa

Jerrett, M., Gale, S., & Kontgis, C. (2010). Spatial Modeling in Environmental and Public Health Research. *International Journal of Environmental Research and Public Health*, *7*(4), Article 4. https://doi.org/10.3390/ijerph7041302

Jiang, X., & Yoo, E. (2018). The importance of spatial resolutions of Community Multiscale Air Quality (CMAQ) models on health impact assessment. *Science of The Total Environment*, *627*, 1528–1543. https://doi.org/10.1016/j.scitotenv.2018.01.228

Keller, C. A., Knowland, K. E., Duncan, B. N., Liu, J., Anderson, D. C., Das, S., Lucchesi, R. A., Lundgren, E. W., Nicely, J. M., Nielsen, E., Ott, L. E., Saunders, E., Strode, S. A., Wales, P. A., Jacob, D. J., & Pawson, S. (2021). Description of the NASA GEOS Composition Forecast Modeling System GEOS-CF v1.0. *Journal of Advances in Modeling Earth Systems*, *13*(4), e2020MS002413. https://doi.org/10.1029/2020MS002413

Lueken, R., Klima, K., Griffin, W. M., & Apt, J. (2016). The climate and health effects of a USA switch from coal to gas electricity generation. *Energy*, *109*, 1160–1166. https://doi.org/10.1016/j.energy.2016.03.078

Malings, C., Tanzer, R., Hauryliuk, A., Saha, P. K., Robinson, A. L., Presto, A. A., & Subramanian, R. (2020). Fine particle mass monitoring with low-cost sensors: Corrections and long-term performance evaluation. *Aerosol Science and Technology*, *54*(2), 160–174. https://doi.org/10.1080/02786826.2019.1623863

Meier, S., Koene, E. F. M., Krol, M., Brunner, D., Damm, A., & Kuhlmann, G. (2024). A lightweight NO_2-to-NO_x conversion model for quantifying NO_x emissions of point sources from NO_2 satellite observations. *Atmospheric Chemistry and Physics*, *24*(13), 7667–7686. https://doi.org/10.5194/acp-24-7667-2024

Pan, S., Yu, W., Fulton, L. M., Jung, J., Choi, Y., & Gao, H. O. (2023). Impacts of the large-scale use of passenger electric vehicles on public health in 30 US. metropolitan areas. *Renewable and Sustainable Energy Reviews*, *173*, 113100. https://doi.org/10.1016/j.rser.2022.113100

Paolella, D. A., Tessum, C. W., Adams, P. J., Apte, J. S., Chambliss, S., Hill, J., Muller, N. Z., & Marshall, J. D. (2018). Effect of Model Spatial Resolution on Estimates of Fine Particulate Matter Exposure and Exposure Disparities in the United States. *Environmental Science & Technology Letters*, *5*(7), 436–441. https://doi.org/10.1021/acs.estlett.8b00279

Pennington, A. F., Cornwell, C. R., Sircar, K. D., & Mirabelli, M. C. (2024). Electric vehicles and health: A scoping review. *Environmental Research*, *251*(Pt 2), 118697. https://doi.org/10.1016/j.envres.2024.118697

Python Release Python 3.10.0. (n.d.). Python.Org. Retrieved March 26, 2025, from https://www.python.org/downloads/release/python-3100/

Richmond-Bryant, J., Owen, R. C., Graham, S., Snyder, M., McDow, S., Oakes, M., & Kimbrough, S. (2017). Estimation of on-road NO2 concentrations, NO2/NOX ratios, and related roadway gradients from near-road monitoring data. *Air Quality, Atmosphere, & Health*, *10*(5), 611–625. https://doi.org/10.1007/s11869-016-0455-7

Rieves, Emma S. & Reid, C. (in preparation). Understanding the impact of modeling choices on $PM_{2.5}$ concentrations using InMAP.

Schnell, J. L., Naik, V., Horowitz, L. W., Paulot, F., Ginoux, P., Zhao, M., & Horton, D. E. (2019). Air quality impacts from the electrification of light-duty passenger vehicles in the United States. *Atmospheric Environment*, *208*, 95–102. https://doi.org/10.1016/j.atmosenv.2019.04.003

Silberstein, J., Mendoza, D., Rieves, E., Reid, C. E., & Hannigan, M. (2024). Investigating the spatiotemporal distribution of fine particulate matter sources during persistent cold air pools in Salt Lake County. *Atmospheric Environment: X*, *24*, 100305. https://doi.org/10.1016/j.aeaoa.2024.100305

Tessum, C. W., Apte, J. S., Goodkind, A. L., Muller, N. Z., Mullins, K. A., Paolella, D. A., Polasky, S., Springer, N. P., Thakrar, S. K., Marshall, J. D., & Hill, J. D. (2019). Inequity in consumption of goods and services adds to racial–ethnic disparities in air pollution exposure. *Proceedings of the National Academy of Sciences*, *116*(13), 6001–6006. https://doi.org/10.1073/pnas.1818859116

Tessum, C. W., Hill, J. D., & Marshall, J. D. (2017). InMAP: A model for air pollution interventions. *PLoS ONE*, *12*(4). https://doi.org/https://doi.org/10.1371/journal.pone.0176131

Visa, M. A., Camilleri, S. F., Montgomery, A., Schnell, J. L., Janssen, M., Adelman, Z. E., Anenberg, S. C., Grubert, E. A., & Horton, D. E. (2023). Neighborhood-scale air quality, public health, and equity implications of multi-modal vehicle electrification. *Environmental Research: Infrastructure and Sustainability*, *3*(3), 035007. https://doi.org/10.1088/2634-4505/acf60d

Vodonos, A., & Schwartz, J. (2021). Estimation of excess mortality due to long-term exposure to PM2.5 in continental United States using a high-spatiotemporal resolution model. *Environmental Research*, *196*, 110904. https://doi.org/10.1016/j.envres.2021.110904

Weis, A., Jaramillo, P., & Michalek, J. (2016). Consequential life cycle air emissions externalities for plug-in electric vehicles in the PJM interconnection. *Environmental Research Letters*, *11*(2), 024009. https://doi.org/10.1088/1748-9326/11/2/024009

World Health Organization. (2025). *Health risks of air pollution in Europe: HRAPIE-2 project: updated guidance on concentration–response functions for health risk assessment of air pollution in the WHO European Region*. https://www.who.int/publications/i/item/9789289062633

Yu, W., Xu, R., Ye, T., Abramson, M. J., Morawska, L., Jalaludin, B., Johnston, F. H., Henderson, S. B., Knibbs, L. D., Morgan, G. G., Lavigne, E., Heyworth, J., Hales, S., Marks, G. B., Woodward, A., Bell, M. L., Samet, J. M., Song, J., Li, S., & Guo, Y. (2024). Estimates of global mortality burden associated with short-term exposure to fine particulate matter (PM2·5). *The Lancet Planetary Health*, *8*(3), e146–e155. https://doi.org/10.1016/S2542-5196(24)00003-2

6 Appendix

Table 4: Age-specific incidence rates for morbidity health endpoints and mortality in Utah and RR for CRFs for each health endpoint

Condition	RR - Point Estimate	RR - 95% CI (low)	RR - 95% CI (high)	Per unit change in pollution (ug/m3)	Beta	Beta (low)	Beta (high)	RR - Age range	Pollutant	Source (RR)	Incidence - Point Estimate	Incidence - 95% CI (high)	Incidence - 95% CI (low)	Source (Incidence)	Age Range - Incidence
Asthma	1.34	1.1	1.63	10	0.01271	0.00414	0.02122	< 18	PM2.5	HRAPIE	471.35327	781.84269	227.37496	GBD	< 20
COPD	1.18	1.13	1.23	10	0.00719	0.00531	0.00899	30+	PM2.5	HRAPIE	1216.46302	1454.38280	965.44045	GBD	30+
IHD event	1.13	1.05	1.22	10	0.00531	0.00212	0.00864	30+	PM2.5	HRAPIE	223.21247	288.72072	172.64864	GBD	30+
Stroke	1.16	1.12	1.2	10	0.00645	0.00492	0.00792	30+	PM2.5	HRAPIE	90.05702	107.02334	75.11354	GBD	30+
Diabetes (Type 2)	1.1	1.03	1.18	10	0.00414	0.00128	0.00719	30+	PM2.5	HRAPIE	607.77821	752.71680	469.94060	GBD	30+
Dementia	1.46	1.2	1.78	10	0.01644	0.00792	0.02504	60+	PM2.5	HRAPIE	868.48624	1000.41336	721.94809	GBD	60+
Autism Spectrum Disorders	1.66	1.23	2.25	10	0.02201	0.00899	0.03522	2 to 12	PM2.5	HRAPIE	376.85572	969.86128	108.67849	GBD	< 14
Lung cancer	1.16	1.1	1.23	10	0.00645	0.00414	0.00899	30+	PM2.5	HRAPIE	113.98623	129.41378	99.40816	GBD	30+
Asthma	1.1	1.05	1.18	10	0.00414	0.00212	0.00719	< 18	NO2	HRAPIE	471.35327	781.84269	227.37496	GBD	< 20
Asthma	1.1	1.01	1.21	10	0.00414	0.00043	0.00828	18+	NO2	HRAPIE	385.03987	487.81406	301.17592	GBD	20+
ALRI	1.09	1.03	1.16	10	0.00374	0.00128	0.00645	< 13	NO2	HRAPIE	491.59667	399.40333	596.62333	GBD	< 14
Mortality	1.1	1.06	1.13	10	0.0041	0.002531	0.00531	all	PM2.5	HRAPIE	615.54	627.56	604.26	GBD	all
Mortality	1.05	1.03	1.07	10	0.0021	0.001284	0.00294	all	NO2	HRAPIE	615.54	627.56	604.26	GBD	all

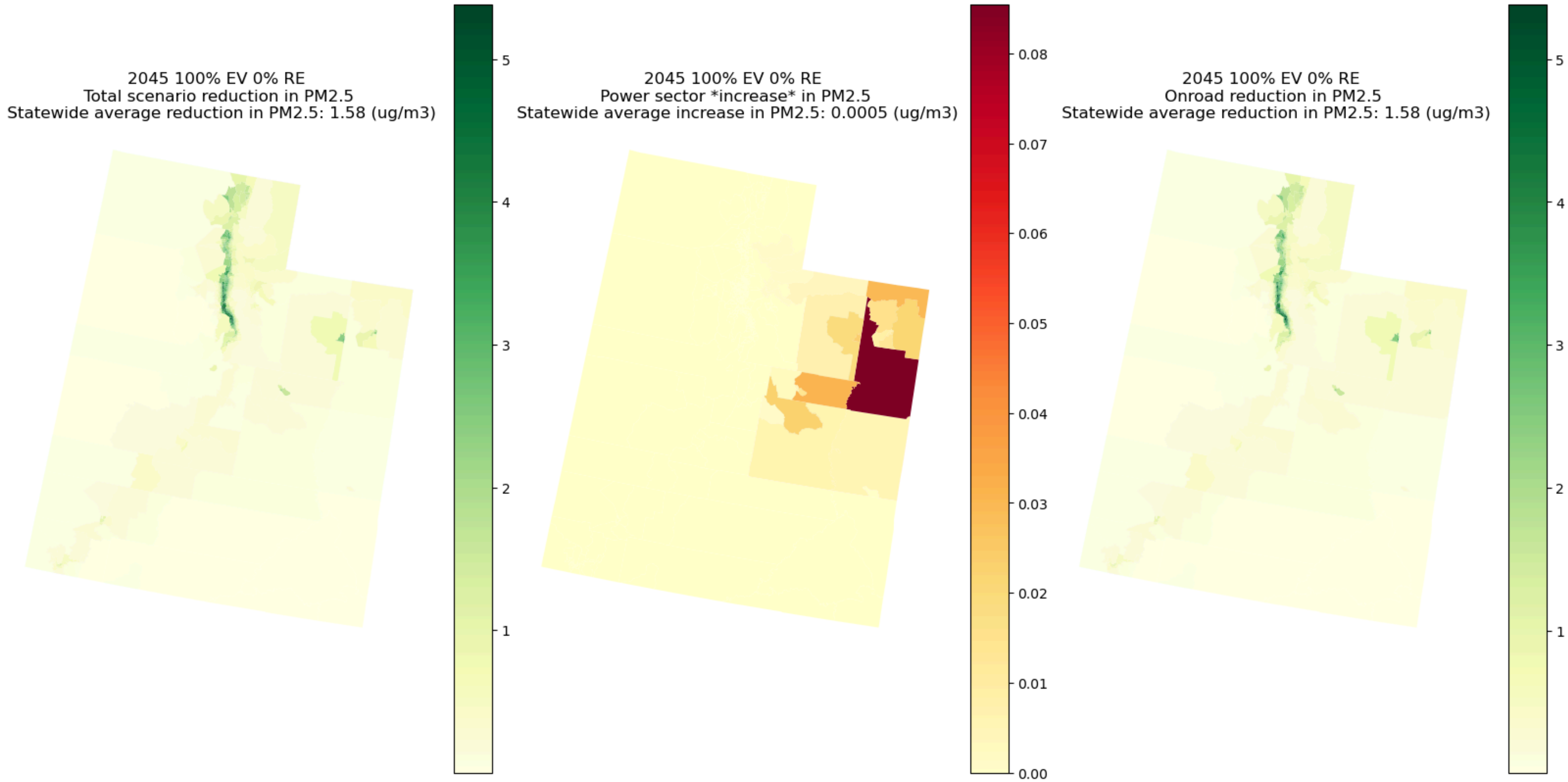

Figure 38: Changes in $PM_{2.5}$ ($\mu g/m^{-3}$) associated with 100% vehicle electrification powered by 0% renewable energy (RE), 2045

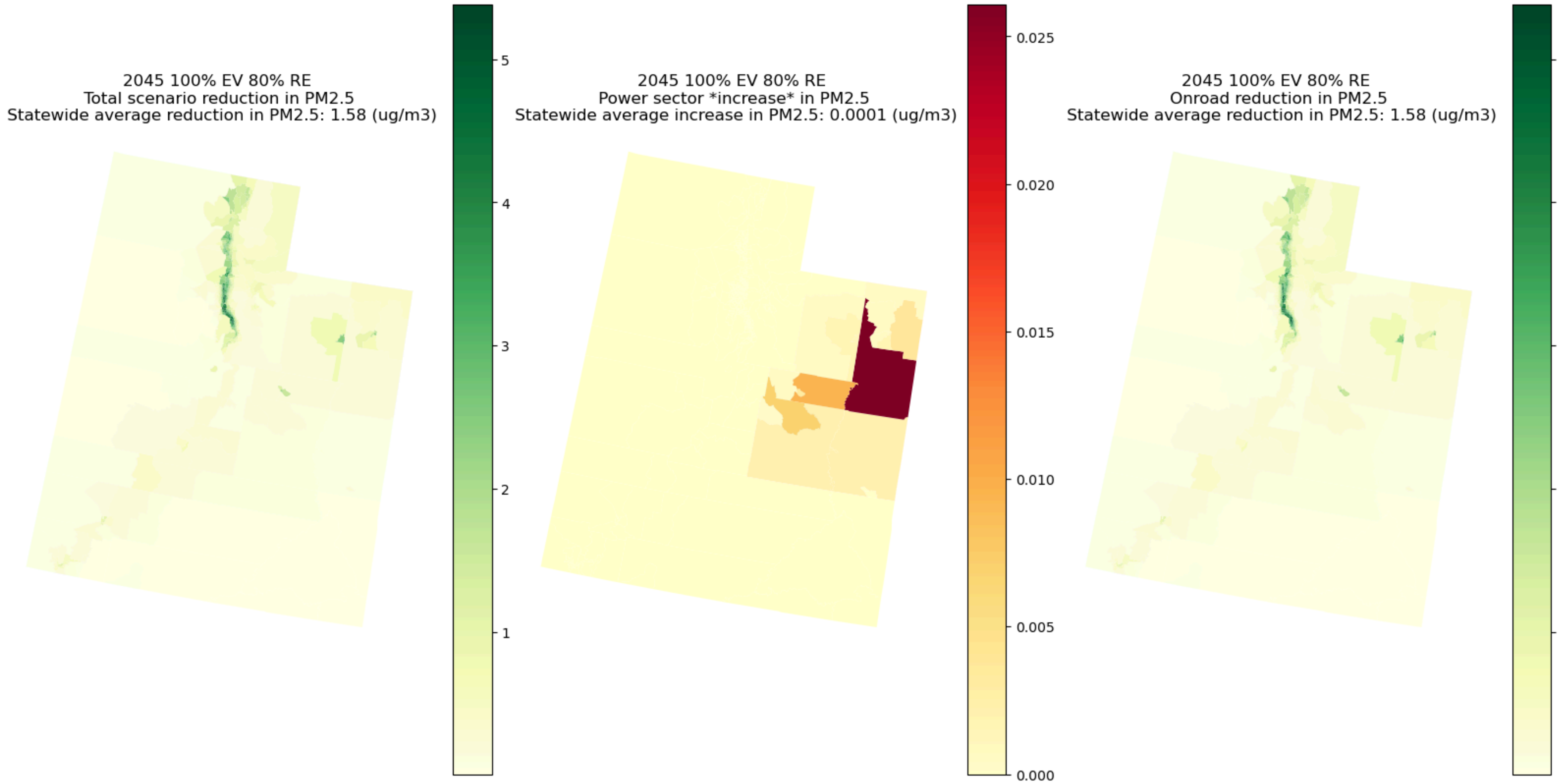

Figure 39: Changes in $PM_{2.5}$ ($\mu g/m^{-3}$) associated with 100% vehicle electrification powered by 80% renewable energy (RE), 2045

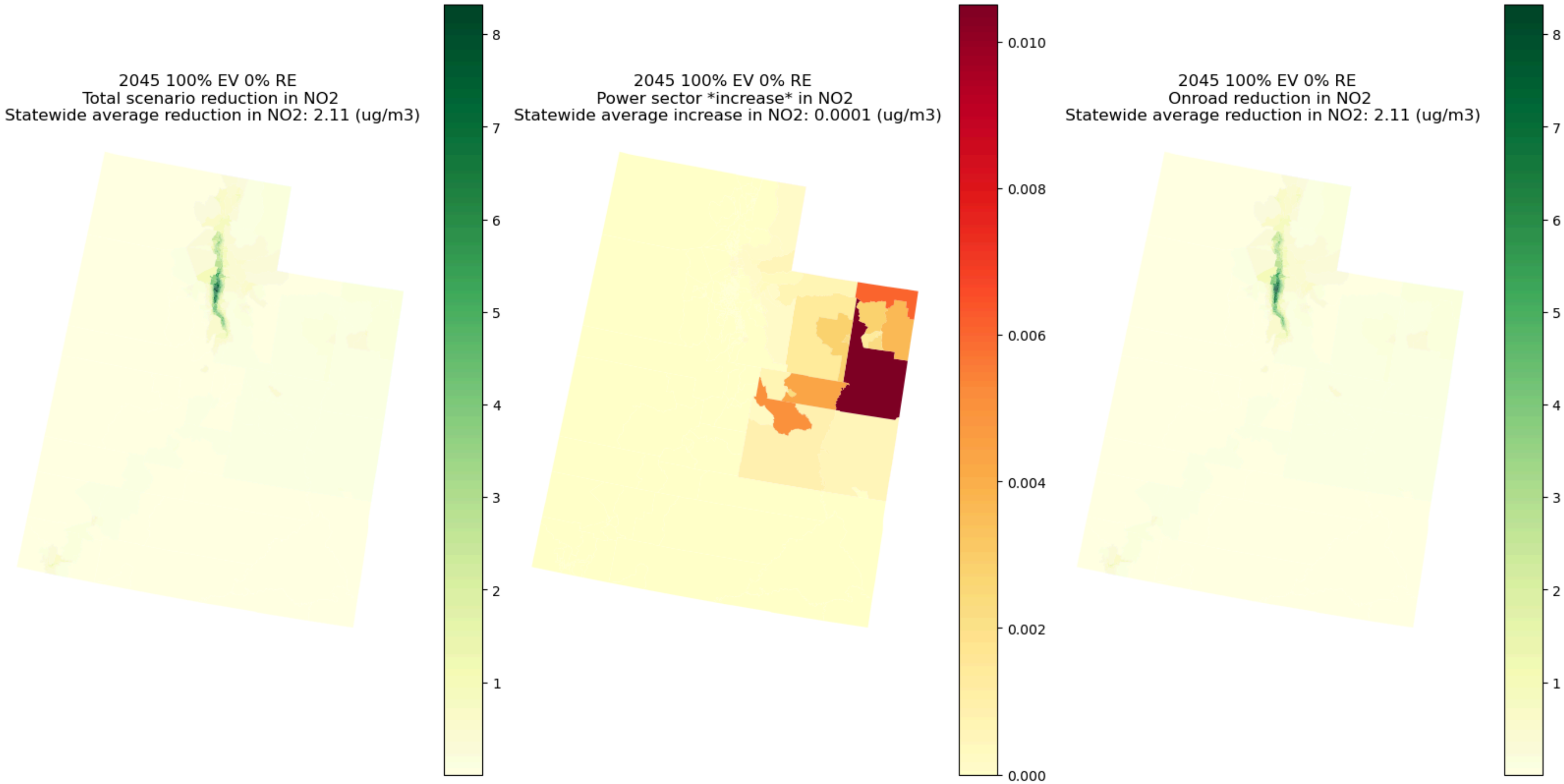

Figure 40: Changes in NO_2 ($\mu g/m^{-3}$) associated with 100% vehicle electrification powered by 0% renewable energy (RE), 2045

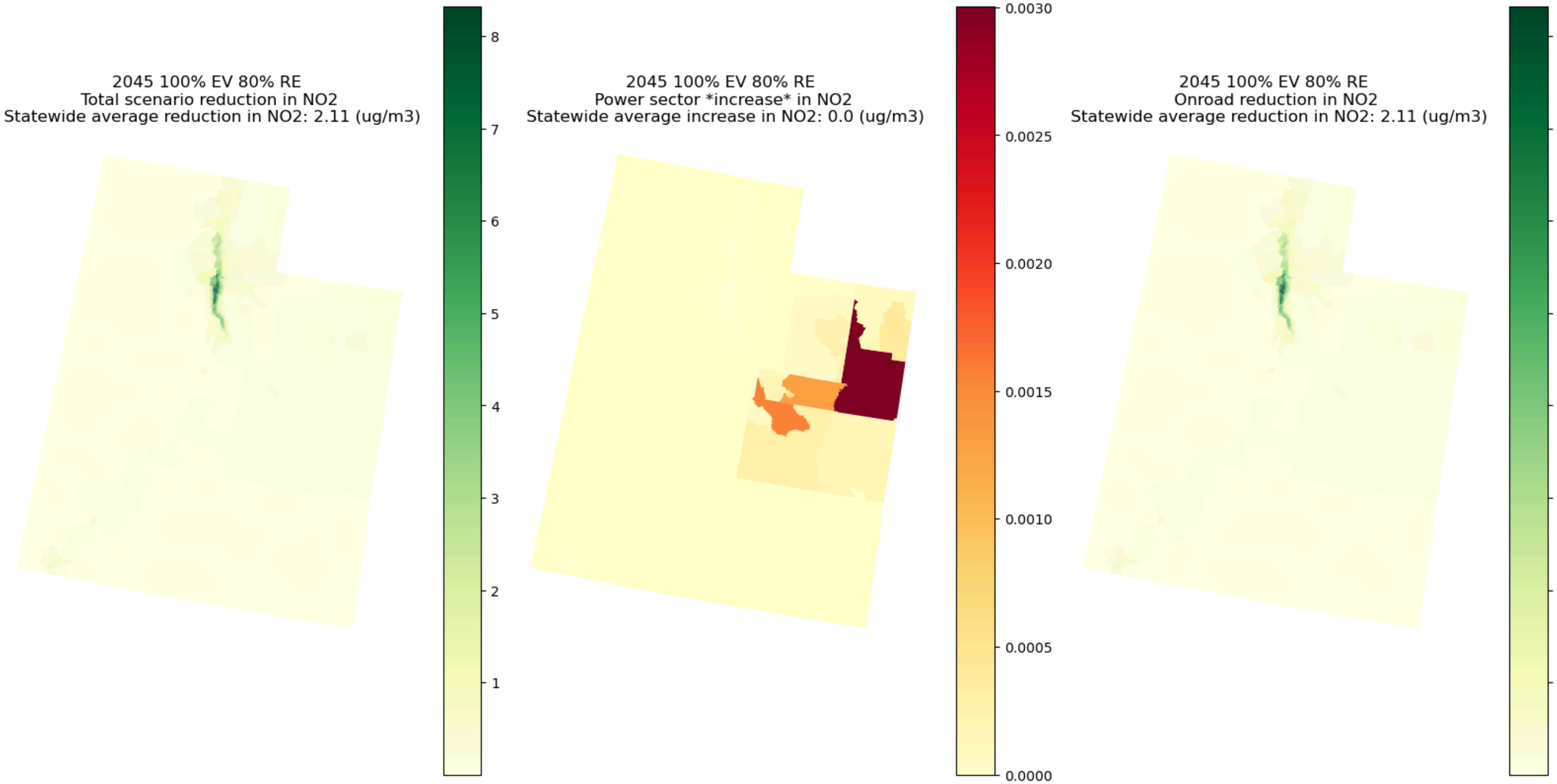

Figure 41: Changes in NO_2 ($\mu g/m^{-3}$) associated with 100% vehicle electrification powered by 80% renewable energy (RE), 2045

Table 5: Results for 100% EV and 0% RE scenarios because these represent the maximum additional generation needs for each scenario year

Scenario year	Added load (TWh)	% Generation in WY	% Generation in UT	% UT Generation - Coal	% UT Generation - Natural gas
2025	20	41%	59%	46%	54%
2035	23.2	35%	65%	36%	64%
2045	26.3	31%	69%	30%	70%